Heliyon 10 (2024) e39911

Contents lists available at ScienceDirect

Heliyon

journal homepage: www.cell.com/heliyon

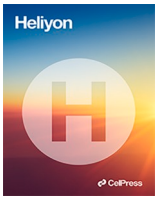

Research article

Chiral amido-oxazoline functionalized MCM-41: A sustainable heterogeneous catalyst for enantioselective Kharasch–Sosnovsky and Henry reactions

Niloofar Tavakoli [a], Hamid Arvinnezhad [b], Shiva Majidian [b], Mahsa Mahramasrar [b], Khosrow Jadidi [a,**], Saadi Samadi [b,*]

[a] Department of Chemistry, Shahid Beheshti University, G.C., Tehran, 1983963113, Iran
[b] Laboratory of Asymmetric Synthesis, Department of Chemistry, Faculty of Science, University of Kurdistan, Sanandaj, 66177-15175, Iran

ARTICLE INFO

Keywords:
Amido-oxazoline ligands
Mesoporous MCM-41
Sustainable heterogeneous catalyst
Enantioselective Kharasch–Sosnovsky reaction
Enantioselective Henry reaction

ABSTRACT

In this study, a series of chiral amido-oxazoline ligands was synthesized with a primary focus on immobilizing the most effective ligands on MCM-41 mesoporous material. Following several attempts, the *para*-nitro group of the chiral amido-oxazoline ligands was successfully reduced to amino group, enabling their immobilization on MCM-41. The resulting chiral heterogeneous amido-oxazoline ligands were characterized using various techniques, including FT-IR, XRD, TGA, SEM, TEM, EDX, and BET-BJH, confirming the successful immobilization of the amido-oxazoline ligands. A comparison of the efficiency of the homogeneous and heterogeneous amido-oxazoline-based ligands in the Kharasch-Sosnovsky and Henry reactions revealed better performance of the heterogeneous ligand. The immobilized amido-oxazoline-copper complexes exhibited remarkable catalytic activity, achieving excellent yields and enantioselectivities (up to 88 % *ee*) in the Kharasch-Sosnovsky reaction, and delivering excellent yields with moderate enantioselectivities in the Henry reaction. Notably, the Henry reaction proceeded with moderate diastereoselectivity, favoring the *syn* diastereomer, under solvent-free conditions, highlighting the sustainability of the process. The heterogeneous nature of the catalysts facilitated effortless recovery and efficient reusability.

1. Introduction

Oxazoline-based ligands have garnered considerable attention in asymmetric transformations due to their significant potential advantages, such as easy accessibility, modular nature, and suitability for a broad range of metal-catalyzed reactions. Typically, this class of ligands can be prepared from readily available chiral β-amino alcohols and carboxylic acids or nitriles, and can be modified by incorporating a diverse range of functional groups. Moreover, the close proximity of the chiral center to the donor nitrogen atom creates a well-organized chiral environment at the catalytic center, which greatly enhances asymmetric induction [1–12].

Introducing sustainable, environmentally friendly, and efficient chiral catalytic systems is a central theme in modern synthetic chemistry. While homogeneous oxazoline-based ligands often exhibit high reactivity and enantioselectivity, their practical application

* Corresponding author.
** Corresponding author.
E-mail address: s.samadi@uok.ac.ir (S. Samadi).

https://doi.org/10.1016/j.heliyon.2024.e39911
Received 13 May 2024; Received in revised form 21 September 2024; Accepted 27 October 2024
Available online 29 October 2024

is mainly hindered by challenges related to separation, recovery, and reuse. The immobilization of oxazoline ligands onto suitable supports provides a reasonable approach to overcoming such limitations, aligning with the principles of sustainability and green chemistry. Mesoporous silica materials such as MCM-41 have emerged as promising supports due to their high surface area, tunable pore size, and ease of functionalization [13–21]. These outstanding features facilitate the immobilization of chiral catalysts, potentially enhancing their performance through confinement effects and site isolation, consequently improving the catalysts' efficiency and significantly impacting enantioselectivity [22–31].

The enantioselective Kharasch-Sosnovsky reaction, which involves the enantioselective oxidation of allylic C-H bonds in olefins primarily using a perester in the presence of a chiral copper complex, is a powerful and cost-effective approach in organic synthesis. This process is distinct from hydroxylation and epoxidation, as a second functional group is formed without altering the C=C bond. Additionally, the resulting chiral allylic ester can be further functionalized to produce a diverse range of products [32–55].

The asymmetric Henry reaction, also referred to as the nitroaldol reaction, is a highly atom-economical process that involves the enantioselective nucleophilic addition of the α-carbon of a nitroalkane to the carbonyl group of an aldehyde or ketone in the presence of a chiral environment, typically involving copper-ligand complexes, resulting in the formation of a C−C bond that consequently yields a chiral β-nitroalcohol [56–83]. The newly formed compounds can be readily transformed into other valuable synthetic intermediates by dehydration to produce nitroalkenes, oxidation of the hydroxy group to produce α-nitro ketones, or reduction of the nitro group to generate β-amino alcohols [84–87]. It is noteworthy that β-amino alcohol derivatives have great potential for the synthesis of important pharmaceutical compounds, such as sphingosine [88], ephedrine [89], and chloramphenicol [89]. Additionally, they have been utilized in the production of β-blockers such as (*S*)-propranolol [90,91], (*S*)-pindolol [92], and (*S*)-metoprolol [93,94], as well as β-receptor agonists such as (−)-denopamine and (−)-arbutamine [95].

Building upon our recent success in utilizing amido-oxazoline ligands **1** for the enantioselective Kharasch-Sosnovsky reaction [96], we aimed to develop a sustainable and recyclable catalytic system by covalently immobilizing amido-oxazoline ligand derivatives on MCM-41. Herein, we report the synthesis and characterization of amido-oxazoline ligands immobilized on MCM-41, and their application in two important enantioselective transformations: the Kharasch-Sosnovsky reaction and the Henry reaction.

2. Result and discussion

2.1. Synthesis of chiral homogeneous amido-oxazoline based ligands

In our previous publication, we described the synthesis of amido-oxazoline ligands **1**. This process begins with the preparation of amino-oxazolines **2** through the reaction of chiral (*S*)-amino alcohols **3** [97] and cyanogen bromide [3–6,96,98–106]. The amino-oxazolines **2** was then reacted with benzoyl chlorides **4** to yield the desired amido-oxazoline ligand derivatives **1**. It was proven that the main structure is oxazolidine-imine form **1′** (Scheme 1) (Pages S2-S5 and Figs. S1-S10, Supplementary Material).

Despite this straightforward strategy, the heterogenization of this class of ligand on MCM-41 poses a challenge. Two practical approaches to covalently immobilize the ligands on MCM-41 mesoporous materials was considered. One strategy involves the introduction of a functional group, such as an amino group, at the *para* position of benzoic acid. The alternative entails the reduction of the nitro group in amido-oxazoline ligands **1** to form an amino group [13–15]. Therefore, to perform the first approach, *para*-amino benzoic acid **5** was chosen as a suitable starting material. Initially, the amino group of benzoic acid **5** was protected using di-*tert*-butyl dicarbonate (Boc_2O) [107,108]. In the ^1H NMR spectrum, the appearance of a singlet signal at $\delta = 1.57$ ppm corresponds to the *tert*-butyl hydrogens. In the subsequent step, similar to the procedure mentioned earlier, the protected benzoic acid **6** was converted to its corresponding benzoyl chloride **7** using oxalyl chloride [96,108]. The resulting benzoyl chloride **7** was then promptly reacted with the amino-oxazolines **2** to produce the desired protected amido-oxazolines **8** (Scheme 2) (Pages S5 and S6, and Figs. S11-S19, Supplementary Material).

Despite numerous attempts, this method did not yield satisfactory results. Therefore, an alternative strategy was employed, in which the protected carboxylic acid **6** was directly reacted with amino-oxazolines **2** using the Appel reagent (PPh_3/CCl_4) [52,109]. This procedure was successful in producing the desired products **8**, achieving significantly higher yields than the previous attempt (Scheme 3). It is apparent that the *in-situ* activation of the carboxylic group led to a remarkable decrease in the formation of unwanted by-products. The presence of signals for aromatic and oxazoline rings at $\delta = 7$–8 ppm and at $\delta = 4$–5 ppm, respectively, in the ^1H NMR spectra confirmed the successful formation of the protected amido-oxazolines **8** (Pages S6 and S7, Supplementary Material).

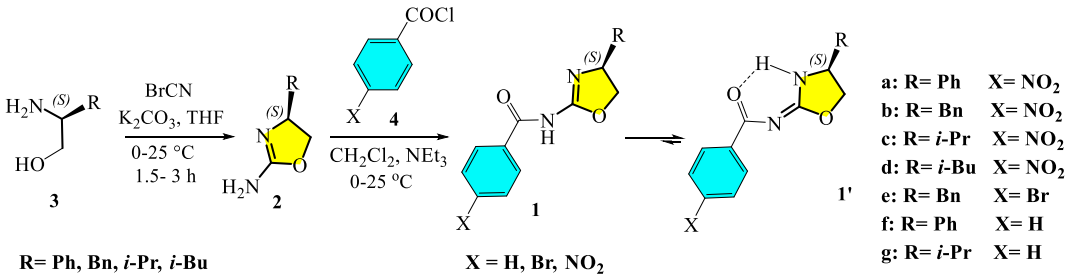

Scheme 1. Synthesis of amido-oxazolines **1**.

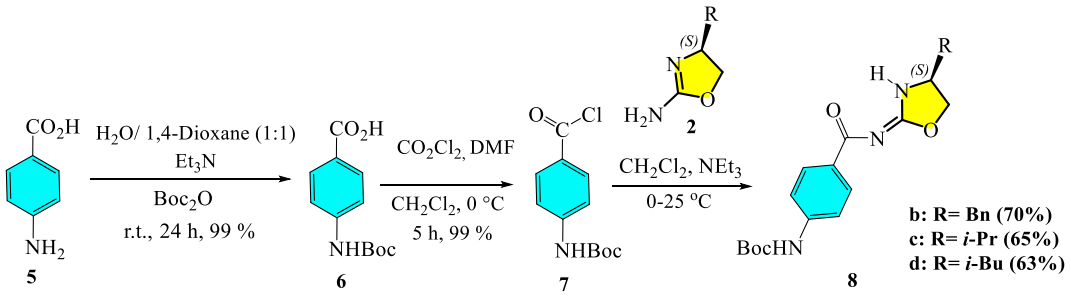

Scheme 2. Preparation of the protected amido-oxazolines **8** from *para*-amino benzoic acid through benzoyl chloride.

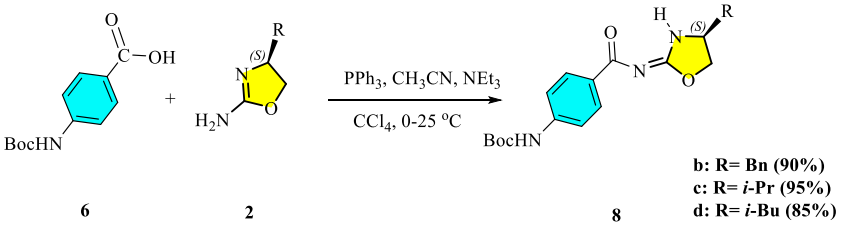

Scheme 3. Preparation of the protected amido-oxazolines **8** from *para*-amino benzoic acid using Appel reagent.

In the final step, amido-oxazolines **8** were treated with trifluoroacetic acid (TFA) to remove the Boc protecting group. However, despite several attempts, the deprotection process was unsuccessful, which is in contrast to our previous study where we effectively eliminated the Boc group [108] (Scheme 4).

As a result of these failures, the second option was explored, involving the reduction of the *para*-nitro group of the amido-oxazolines **1** into an amino group. Our previous experiments revealed that the use of hydrogen gas in the presence of a catalytic amount of Pd/C (10 %) is the most effective method for reducing nitro groups [109,110] (Scheme 5). This procedure can provide the corresponding aniline-oxazoline ligands **9** in 97 % and 93 % yield, respectively (Pages S7 and S8, and Figs. S20-S27, Supplementary Material). In the ^{1}H NMR spectra of compound **1a**, the *ortho* and *meta* protons appeared at $\delta = 8.41$ ppm and 8.26 ppm, respectively, while in **9a**, these protons shift to $\delta = 6.65$ ppm and 8.09 ppm, respectively. In fact, in the ^{1}H NMR spectra of compounds **1a** and **1b**, the *ortho* protons appeared at downfield values, while in compounds **9a** and **9b**, the *meta* protons are observed in downfield regions.

2.2. Heterogenization of the synthesized chiral amido-oxazoline ligands

Based on our previous study [96], which found that the amido-oxazoline ligands **1** containing phenyl and benzyl groups on the oxazolidine ring, demonstrated the highest efficiency, we opted to immobilize them on cylindrical MCM-41 mesoporous support. Initially, MCM-41 silica was synthesized hydrothermally, utilizing sodium silicate as a silica source and tetradecyl trimethyl ammonium bromide (TTAB) as a template agent to regulate pore size [18,108].

To immobilize the aniline-oxazoline ligands **9** on the MCM-41, it is essential to have a linker between the support and the ligand. Therefore, the mesoporous silica was reacted with 3-chloropropyltrimethoxysilane (CPTMS) as a linker to create Cl-MCM-41 material. In the subsequent step, the prepared aniline-oxazoline ligands **9a** and **9b** were treated with the Cl-MCM-41 in refluxing toluene (Page S8, Supplementary Material). During this process, the chloro group is replaced with the amino group, resulting in the formation of heterogeneous oxazoline based ligands **10** (OX-R-MCM-41) [98,108,111] (Scheme 6).

2.3. Characterization of the chiral heterogeneous ligands 10

Various techniques were employed to study the structure of the prepared chiral heterogeneous ligands **10**. These methods included Fourier transform infrared spectroscopy (FT-IR), powder X-ray diffraction (XRD), thermogravimetric analysis (TGA), differential

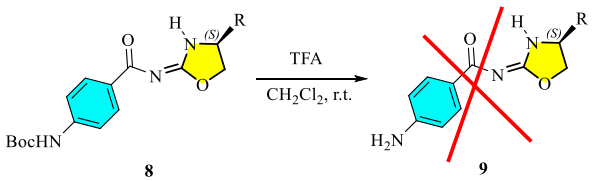

Scheme 4. Unsuccessful deprotection of Boc group from the protected amido-oxazolines **8**.

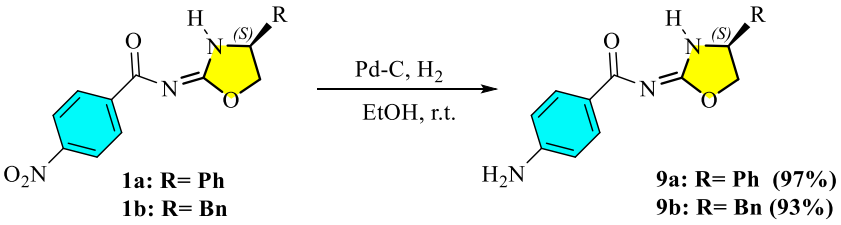

Scheme 5. Direct conversion of the nitro group of amido-oxazolines **1** into amino group using H_2, Pd/C.

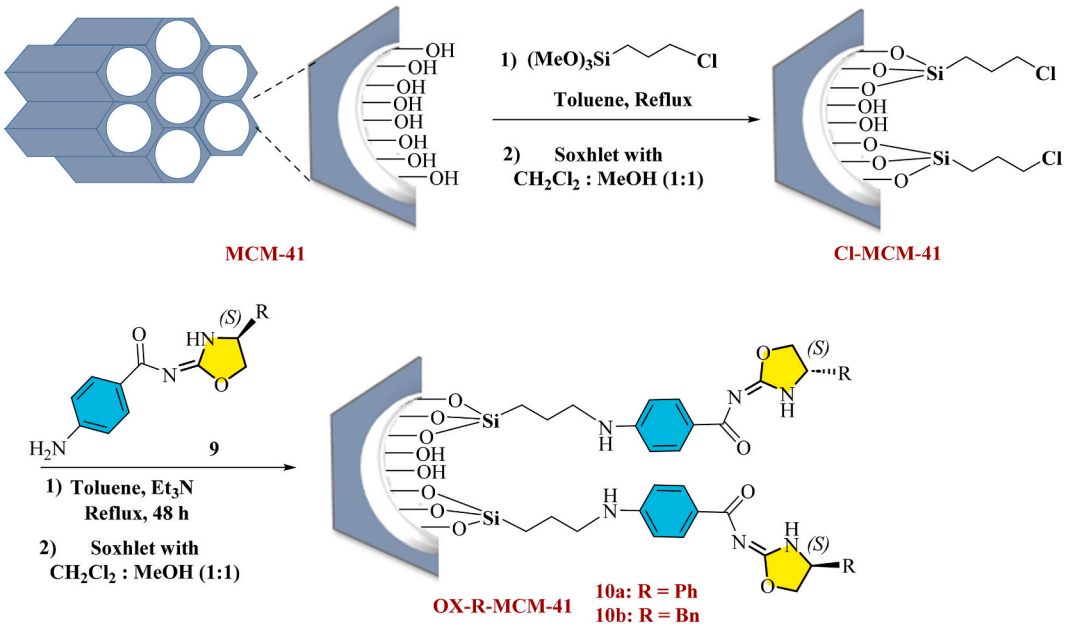

Scheme 6. Immobilization of the aniline-oxazoline ligands **9** on mesoporous MCM-41.

thermal analysis (DTA), CHN elemental analysis, scanning electron microscopy (SEM), energy dispersive X-ray analysis (EDX), transmission electron microscopy (TEM), and BET/BJH nitrogen adsorption-desorption methods.

The results of the experimental analysis indicated that the aniline-oxazoline ligands **9** were successfully immobilized on the MCM-41. A comparison of the FT-IR spectra of MCM-41, Cl-MCM-41, and the chiral heterogeneous ligands **10** (OX-Ph-MCM-41 **10a** and OX-Bn-MCM-41 **10b**) showed notable differences in their respective spectra (Fig. 1).

The FT-IR spectrum of MCM-41 exhibited the following spectral characteristics: A broad band observed at 3430 cm^{-1} indicated the stretching vibration of O-H bonds in adsorbed water, accompanied by O-H bending vibration at 1634 cm^{-1}. The bands around 1221 and 1084 cm^{-1} were identified as the asymmetric stretching of the Si-O-Si group, while the symmetric stretching modes of the Si-O-Si group were observed at 809 and 591 cm^{-1}. The presence of Si-OH groups was indicated by a band at 956 cm^{-1}, and an absorption band at 451 cm^{-1} corresponded to the bending vibration of Si-O-Si groups.

In the FT-IR spectrum of Cl-MCM-41, a distinctive absorption band at 707 cm^{-1} indicated the stretching of the C-Cl bond. Absorption bands at about 2953 and 2864 cm^{-1} corresponded to the asymmetric and symmetric stretching vibrations of C-H bonds in the CH_2 groups of the propyl chain. Additionally, the intensity of the broad band at around 3400 cm^{-1} is decreased, confirming the attachment of CPTMS on the mesoporous MCM-41.

The FT-IR spectra of the chiral heterogeneous ligands **10** exhibit characteristic vibrational bands indicative of the presence of functional groups. These bands are typically observed at around 1700 cm^{-1} and correspond to the stretching vibrations of C=N and C=O groups present in the oxazoline ligands. Broad bands around 3400 cm^{-1} correspond to the N-H groups of the oxazoline. These bands are a clear indication of the successful immobilization of the oxazoline ligands on the MCM-41. It is worth noting that distinct bands in the ranges of 1000–1250 cm^{-1} and 450-950 cm^{-1} were observed in all of the materials analyzed [108,111].

The powder XRD pattern of the synthesized mesoporous MCM-41 showed the presence of four distinct peaks at low angle of 2θ. The peak at (1 0 0) was particularly striking, exhibiting a significantly higher intensity in comparison to the other peaks such as (1 1 0), (2 0 0), and (2 1 0), which displayed relatively lower intensities [108,111] (Fig. 2).

These characteristic peaks collectively confirm the creation of a well-structured hexagonal mesoporous substance with a p6mm space group [112]. The XRD patterns of the Cl-MCM-41 and the chiral heterogeneous ligands **10** displayed a general decrease in

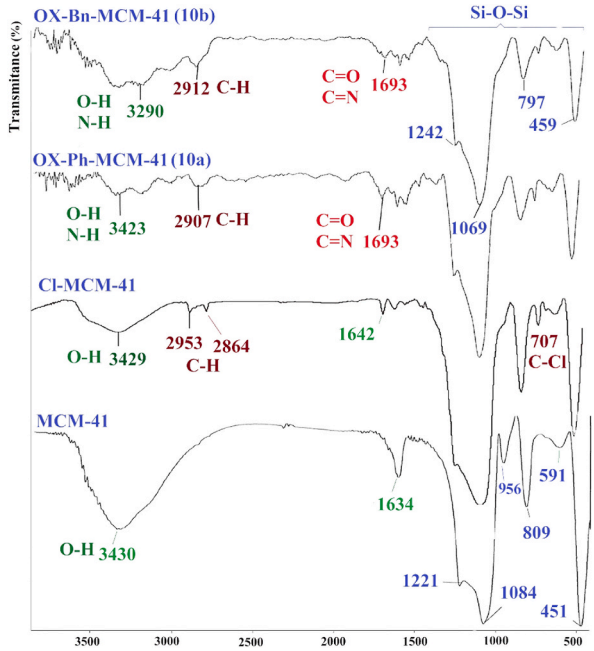

Fig. 1. The FT-IR spectra of MCM-41, Cl-MCM-41, and chiral heterogeneous ligands **10**.

intensity of the peaks, potentially due to the contrast matching between the organic moieties that are integrated into the mesoporous channels of MCM-41 and the silica framework. However, the organic functionalization did not significantly alter the hexagonal structure of the channels. The lower intensity of OX-Ph-MCM-41 **10a** compared to OX-Bn-MCM-41 **10b** is likely attributed to a greater quantity of the aniline-oxazoline ligand **9a** being immobilized on the MCM-41 than **9b**.

The amounts of the immobilized the aniline-oxazoline ligands **9a** and **9b** on the MCM-41 were determined using thermogravimetric analysis (TGA) and CHN elemental analysis. The TGA diagrams showed that the chiral heterogeneous ligands **10a** and **10b** experienced significant weight loss between 150 and 600 °C, as illustrated in Fig. 3. Minor weight losses of around 1–2 wt% at temperatures below 150 °C were due to the elimination of physically adsorbed water. Additionally, the DTA analysis revealed a two-step weight loss at around 380 °C and 555 °C as a result of the oxazoline decomposition. The findings confirmed that the aniline-oxazoline ligands **9a** and

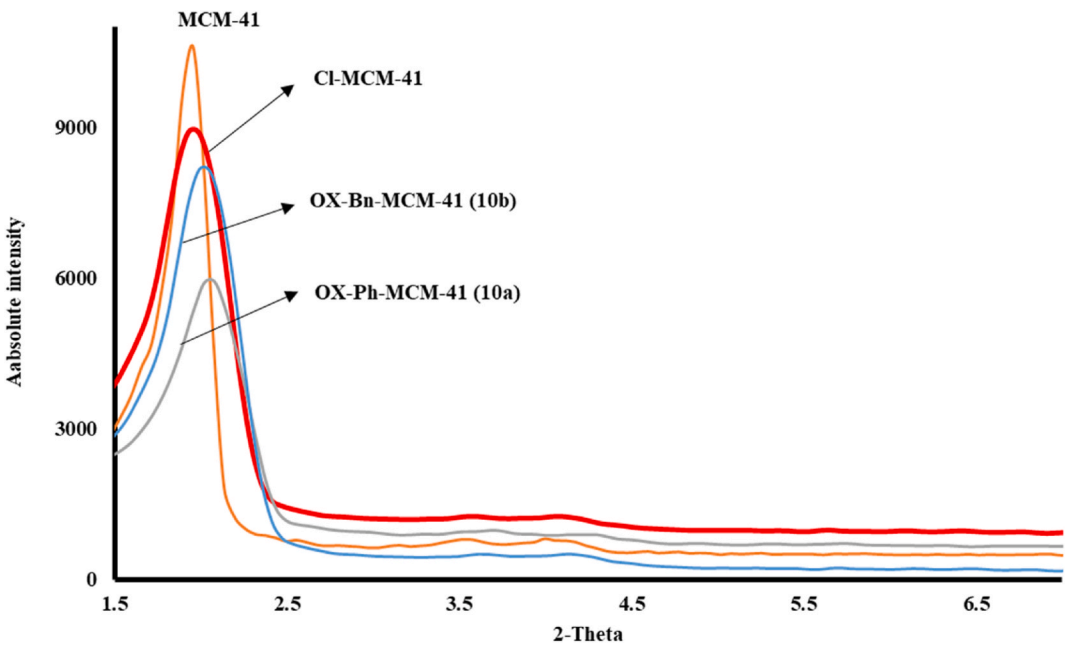

Fig. 2. The XRD patterns of MCM-41, Cl-MCM-41, and chiral heterogeneous ligands **10**.

9b are covalently bonded to the MCM-41 and demonstrated thermal stability up to 380 °C. Furthermore, the CHN elemental analysis revealed that the amounts of ligands **9a** and **9b** attached on the MCM-41 are nearly 0.5 mmol/g and 0.3 mmol/g, respectively.

Fig. 4 displays scanning electron micrographs (SEM) of the MCM-41, the Cl-MCM-41 and the chiral heterogeneous ligands **10**, aiming to examine potential morphological alterations. The analysis of the SEM images reveals that there are no noticeable differences in the size and morphology of the material before and after the immobilization of the aniline-oxazoline ligands **9**.

Immobilization of the synthesized chiral ligands **9a** and **9b** on the MCM-41 was also confirmed using the EDX spectrum (Fig. 5). The presence of nitrogen and carbon elements serves as confirmation for the efficient immobilization of the ligands. It is worth noting, however, that the presence of chlorine suggests that there are still some unreacted linkers remaining.

The TEM micrograph of the chiral heterogeneous ligand **10a** revealed the presence of a hexagonal structure, as shown in Fig. 6.

The specific surface areas (S_{BET}) of the chiral heterogeneous ligands **10a** and **10b** were determined using the BET method. The pore diameter at the peaks of the pore size distributions (D_p) was derived from the adsorption branches of the isotherms, employing Barrett-Joyner-Halenda (BJH) method; and the total pore volumes (V_p) were obtained based on the nitrogen uptake amount at a p/p_0 value of 0.99.

The summarized data can be found in Table 1. It was observed that all of the parameters decreased from the MCM-41 to the Cl-MCM-41 and to the chiral heterogeneous ligands **10**, suggesting pore blocking caused by the linker and oxazoline ligands overloading. The chiral heterogeneous ligand **10a** exhibited higher overloading compared to **10b**, as previously confirmed through CHN and low-angle XRD analysis, which led to a decrease in specific surface area, lower total pore volumes, and narrower pore size distributions.

Fig. 7 presents the nitrogen adsorption-desorption isotherms of the chiral heterogeneous ligands **10a** and **10b**. The isotherms demonstrate a type IV behavior with H_4 hysteresis loops, indicating the presence of a narrow slit mesoporous structure, as classified by IUPAC [113]. The heterogeneous materials **10** display two distinct capillary condensation steps at low and high relative pressures. In the case of mesoporous structure **10a**, capillary condensation occurs within the range of approximately $0.01 < p/p_0 < 0.30$, and another condensation step is observed around $0.82 < p/p_0 < 0.99$. This structure exhibits an H_4 hysteresis loop spanning from approximately $p/p_0 = 0.25$ to 0.95. Conversely, mesoporous structure **10b** demonstrates capillary condensations at nearly $0.01 < p/p_0 < 0.25$ and another at approximately $0.90 < p/p_0 < 0.99$. Moreover, it displays an H_4 hysteresis loop within the range of approximately $p/p_0 = 0.1$ to 0.99. The pore size distribution curve, shown in Fig. 8, demonstrates a narrow distribution of pore sizes for mesoporous structure **10a**.

2.4. Catalytic activity of the copper complexes of homogenous and heterogeneous amido-oxazoline ligands

2.4.1. Examination of the catalysts in the enantioselective Kharasch-Sosnovsky reaction

Based on our previous studies in the enantioselective Kharasch-Sosnovsky reaction, it has been firmly established that the inclusion of mesoporous additives has a profound influence on the overall outcomes, especially in terms of enantioselectivity [108,109,114]. Therefore, before studying the catalytic activity of the prepared heterogeneous catalysts, the homogeneous ones were investigated in the presence of mesoporous MCM-41 as an additive (Fig. 9).

To carry out the homogeneous reaction, cyclohexene was enantioselectively oxidized using *t*-butyl *p*-nitroperbenzoate **11a** [96] in the presence of oxazoline ligands **1**, **8**, and **9**, $Cu(CH_3CN)_4PF_6$, a highly effective copper source for this transformation [96,108,109,114] and a catalytic amount of phenyl hydrazine as a reducing agent to regenerate Cu(I) [96,108,114].

Based on Fig. 9, it can be inferred that the homogeneous catalysts with electron-withdrawing groups (EWG), such as NO_2, and Br on the phenyl ring, exhibited higher enantioselectivity (Fig. 9, Ligands **1a-e**). These results align with our previous research [96], which identified amido-oxazoline ligands containing a NO_2 group as the most effective. In contrast, the catalysts with NH_2, an electron-releasing group (ERG), displayed the lowest enantioselectivity and yield (Fig. 9, Ligands **9a** and **9b**), requiring three times the reaction time compared to the NO_2-containing catalysts (Fig. 9, Ligands **1a-d**). Catalysts with no substituent or an NHBoc group demonstrated efficiency lower than those with EWGs but higher than those with an NH_2 group (Fig. 9, Ligands **1f, 1g** and **8b-d**). It should be noted that the catalysts with a phenyl or benzyl group on the oxazoline ring outperformed those with *i*-propyl or *i*-butyl

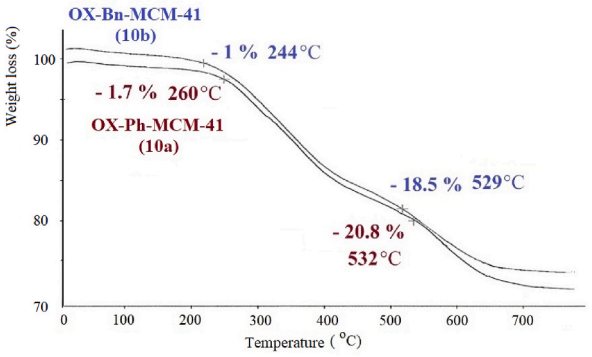

Fig. 3. The TGA of chiral heterogeneous ligands **10**.

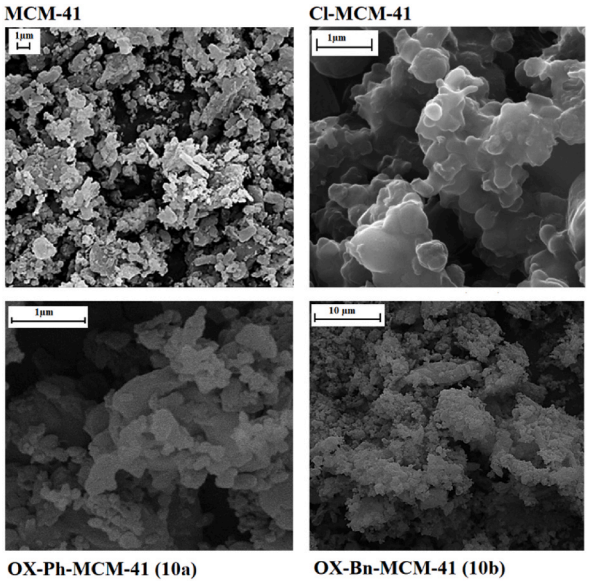

Fig. 4. SEM images of MCM-41, Cl-MCM-41, and chiral heterogeneous ligands **10**.

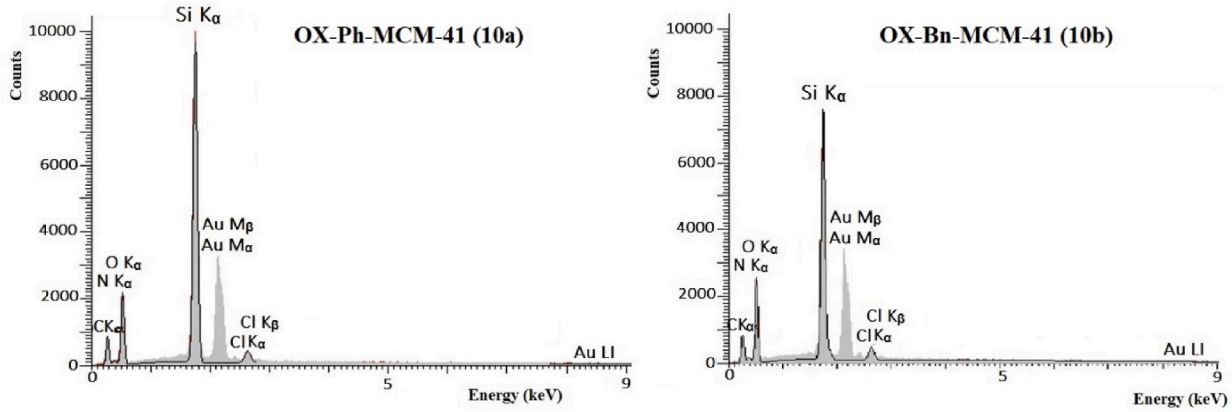

Fig. 5. The EDX spectra of chiral heterogeneous ligands **10**.

substitutions (Pages S8 and S9, Supplementary Material).

Moreover, the experimental evaluation of other cyclic and acyclic olefins under these conditions provided results similar to our prior findings [96,98]. Following the above experiments, the efficacy of the prepared heterogeneous catalysts was evaluated using various peresters (as depicted in Fig. 10) under similar conditions.

It is noteworthy that while the homogeneous catalyst with the NH_2 group produced the poorest results (Fig. 9, Ligands **9a** and **9b**), the corresponding immobilized catalysts on the MCM-41 demonstrated outstanding enantioselectivity and yield. Remarkably, the heterogeneous catalysts 10a-Cu(I) and 10b-Cu(I) gave even more favorable results than the homogeneous ones (Fig. 9 vs. Fig. 10).

A comparison of the efficiency of the heterogeneous catalysts **10a**-Cu(I) and **10b**-Cu(I) showed that while the use of heterogeneous catalyst **10a**-Cu(I), containing phenyl groups at the oxazoline rings, generally gave the best results, it typically required a longer reaction time. In general, under optimized conditions, the conversion of cyclohexene to enantioenriched (*S*)-allylic ester using *t*-butyl *p*-nitroperbenzoate **11a** in the presence of heterogeneous catalyst **10a**-Cu(I) led to remarkable enantioselectivity of 86 % and a high yield of 92 % within a 48-h timeframe.

Furthermore, in line with our prior researches [96,108,109,114] employing peresters containing EWGs (Fig. 10, X' = NO_2, Cl) led to the formation of chiral allylic esters with higher enantioselectivity and yield in a shorter time compared to those with ERGs (Fig. 10, X' = Me, OMe). In other words, there is a direct relationship between the strength of the EWGs on the perester and the enantioselectivity and yield of the reaction, meaning that an increase in the former leads to an improvement in the latter.

With optimized reaction conditions in hand, the generality of this protocol was investigated using other cyclic and acyclic olefins. The experimental data presented in Table 2 revealed that, under these conditions, both heterogeneous catalysts (**10a**-Cu(I) and **10b**-Cu

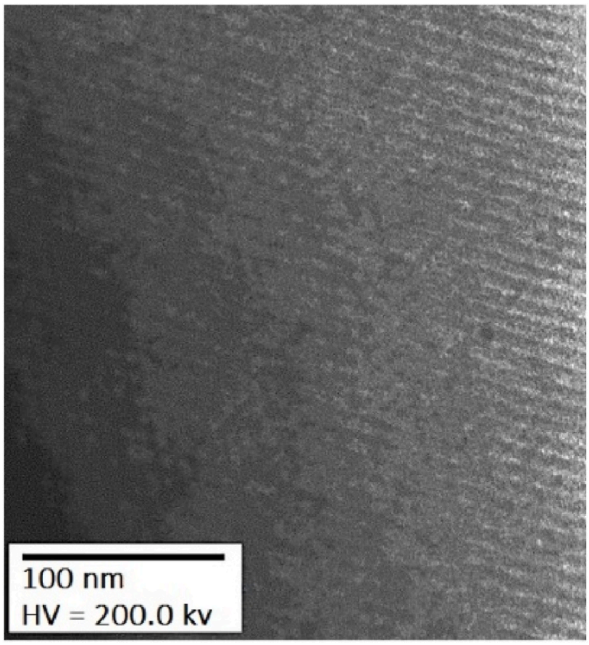

Fig. 6. TEM image of chiral heterogeneous ligand **10a**.

Table 1
Textural properties of MCM-41, Cl-MCM-41, and chiral heterogeneous ligands **10**.

Sample	S_{BET} (m^2/g)[a]	V_p (cm^3/g)[b]	D_p (nm)[c]
MCM-41	1105	1.14	4.32
Cl-MCM-41	543	0.623	3.17
10a	229	0.188	2.40
10b	397	0.3903	2.93

[a] S_{BET} is the surface area calculated from the BET equation.
[b] V_p is the pore volume determined from the adsorption branch of the isotherm at $p/p_0 = 0.99$.
[c] D_p represents the pore diameter calculated using the BJH method.

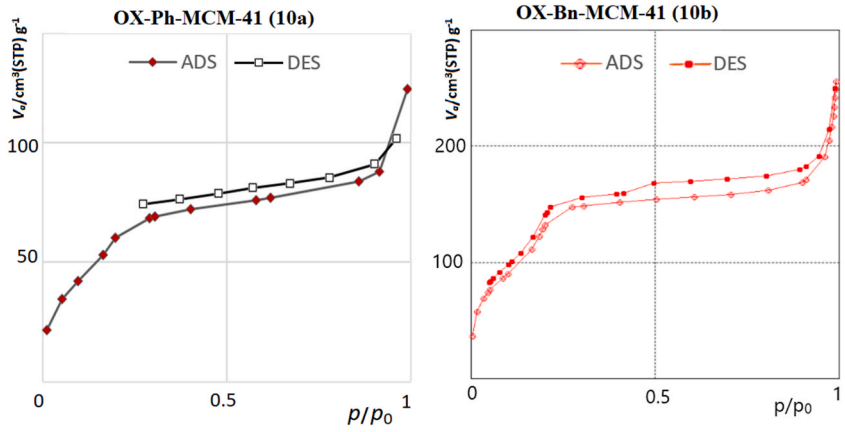

Fig. 7. The nitrogen adsorption–desorption isotherms of chiral heterogeneous ligands **10** at 77 K.

(I)) exhibited good efficiency for the studied substrates. Notably, allylic oxidation of 1,5-cyclooctadiene (1,5-COD) yielded better results than other olefins (entries 7 and 8). This reaction proceeded with the shortest reaction time, producing the (*S*)-enantiomer of the allylic ester product with the highest enantioselectivity and yield in comparison to other olefin substrates. This behavior can be linked to the catalyst complex cavity, which can effectively accommodate the twist-boat conformation of 1,5-COD [115–117].

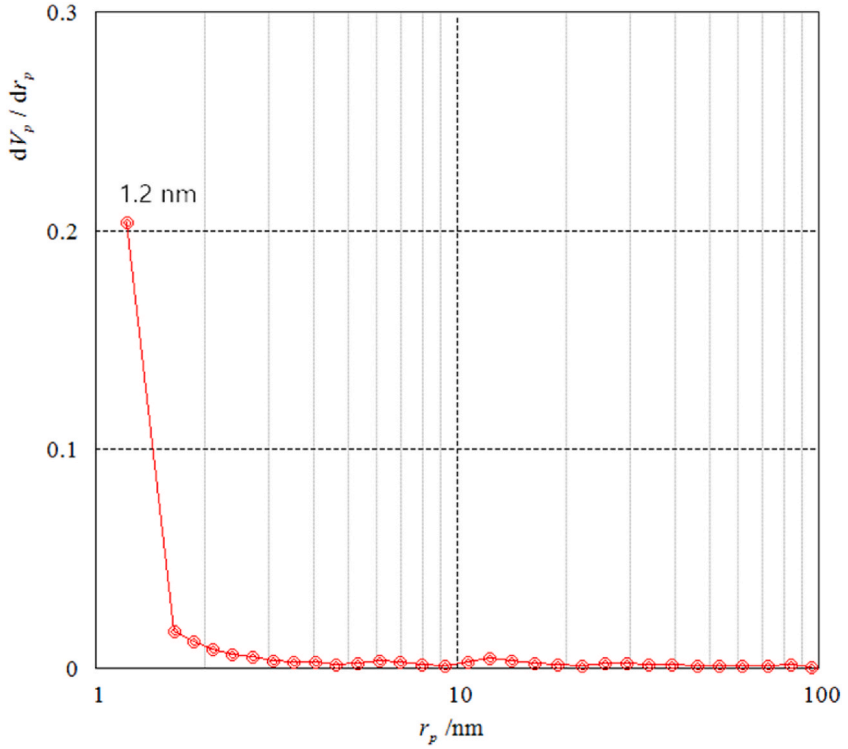

Fig. 8. Pore size distribution curve of chiral heterogeneous ligand **10a**.

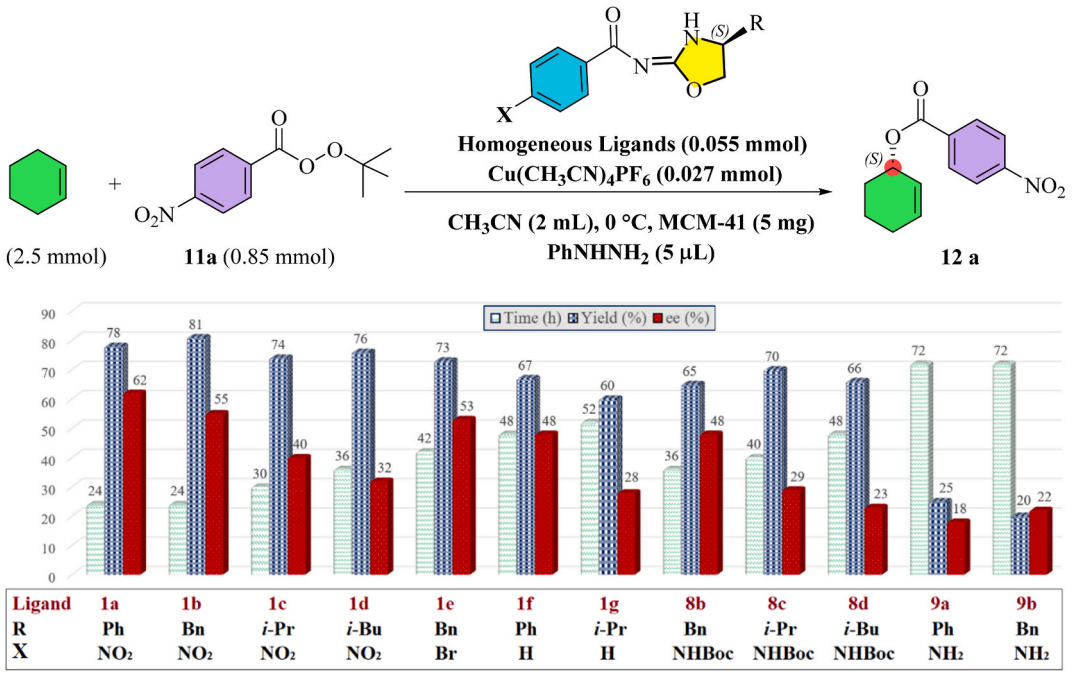

Fig. 9. Enantioselective allylic oxidation of cyclohexene using the chiral homogeneous oxazoline-copper(I) complexes.

Additionally, consistent with our expectations [12,96,98,118], the cyclic substrates produced higher enantioselectivity and yield in a shorter reaction time compared to the acyclic ones (Table 2, entries 1–8 vs. 9–14). The observed remarkable differences between cyclic and acyclic olefins can be attributed to the steric congestion encountered by the cyclic reactants at the key intermediate stage of

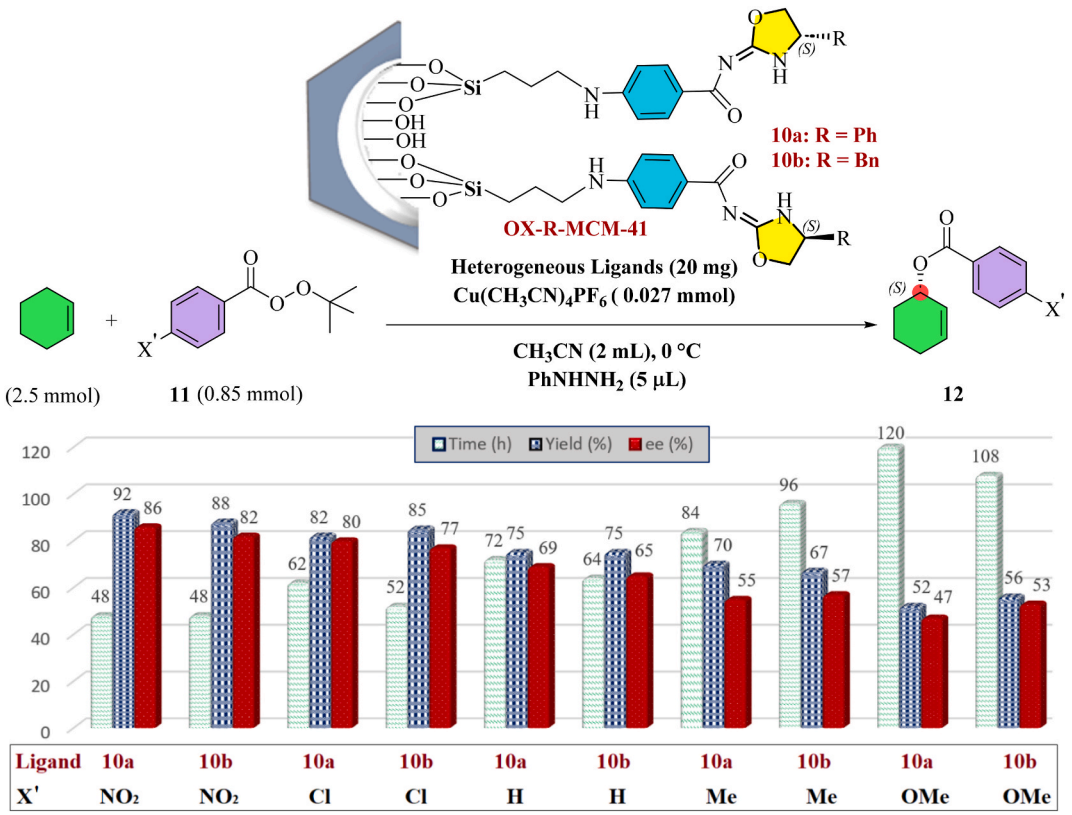

Fig. 10. Comparison of the efficiency of the chiral heterogeneous catalysts using different peresters in the enantioselective allylic oxidation of cyclohexene.

Table 2
Enantioselective copper catalyzed allylic oxidation of olefins using heterogeneous oxazoline based ligands.

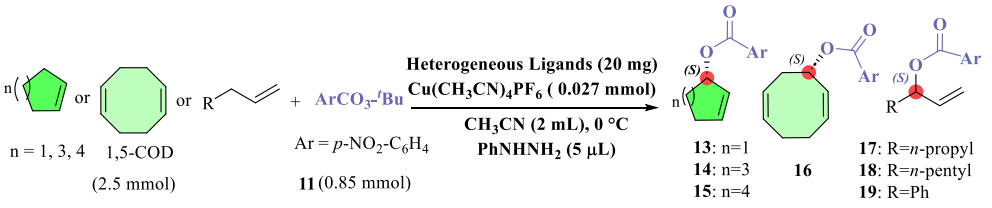

Entry	Olefin	Heterogeneous Ligand	Allylic Ester	Time (h)	Yield (%)	*ee* (%)
1	Cyclopentene	**10a**	13	55	84	68
2	Cyclopentene	**10b**	13	52	77	71
3	Cycloheptene	**10a**	14	65	86	77
4	Cycloheptene	**10b**	14	60	90	68
5	Cyclooctene	**10a**	15	72	72	62
6	Cyclooctene	**10b**	15	72	65	65
7	1,5-COD	**10a**	16	34	95	88
8	1,5-COD	**10b**	16	34	95	83
9	1-Hexene	**10a**	17	132	42	28
10	1-Hexene	**10b**	17	108	35	33
11	1-Octene	**10a**	18	148	30	27
12	1-Octene	**10b**	18	148	33	22
13	1-Allyl benzene	**10a**	19	156	37	32
14	1-Allyl benzene	**10b**	19	156	29	26

the reaction. In contrast, acyclic olefins exhibit higher flexibility, allowing them to easily overcome the steric hindrance caused by the oxazoline ring by adopting a wide range of geometries [12].

Based on literature [119–127], the proposed mechanism of the reaction involves the complexation of the heterogeneous oxazoline based ligands **10** with Cu(I) to form a chiral catalyst. It is hypothesized that the chiral catalyst predominantly coordinates with cyclohexene, resulting in the formation of complex **I** (Scheme 7) [128].

The addition of perester **11** initiates the reaction through a catalytic cycle that induces changes in the copper oxidation state. In the first step, cyclohexene undergoes substitution by perester **11**. Subsequently, an oxidative-addition step occurs where the concerted cleavage of the oxygen-oxygen bond in perester **11** generates a crypto-*tert*-butoxyl radical and oxidizes Cu(I) to Cu(III). Following this, cyclohexene once again coordinates with the Cu(III). Then, in the rate-determining step, an intramolecular process takes place wherein the *tert*-butoxy group bonded to the copper complex selectively removes a prochiral allylic hydrogen from cyclohexene. Consequently, the elimination of *tert*-butyl alcohol leads to the formation of a key intermediate. A subsequent attack by carboxyl on the *Si*-face of cyclohexenyl triggers a pericyclic rearrangement involving the migration of the π-bond and stereospecific reductive-elimination step. Eventually, upon substitution with cyclohexene, Cu(I)-cyclohexene is regenerated, resulting in the release of the enantioenriched (*S*)-allylic ester **12**.

2.4.2. Examination of the catalysts in the enantioselective Henry reaction

To further investigate the effectiveness of the prepared heterogeneous catalysts, they were also examined in the enantioselective Henry reaction (Table 3) [77,129,130]. Initially, the reaction between *p*-chloro benzaldehyde and nitromethane was conducted at room temperature in toluene, using Et_3N as a base, in the presence of a catalytic amount of the heterogeneous ligand containing phenyl group (**10a**) and $Cu(CH_3CN)_4PF_6$ (Table 3, entry 1). The reaction under these conditions resulted in the production of enantioenriched (*S*)-*β*-nitroalcohol **20a** with low yield and enantioselectivity, and the reaction time was lengthy, taking 40 h to complete (Pages S9 and S10, and Figs. S28-S32, Supplementary Material).

To improve the yield and enantioselectivity of the product, various factors were investigated in this reaction, including the effects of solvent, base, temperature, Cu salt, and the heterogeneous ligand. By testing the reaction in polar and non-polar solvents, it was found that protic solvents, especially EtOH, enhanced both enantioselectivity and yield (Table 3, entries 1–7). However, the most favorable results were obtained under solvent-free conditions, where the reaction time decreased, and the enantioselectivity and yield of the chiral product were significantly improved (Table 3, entry 8).

When testing various bases, including tetramethylguanidine, *N*, *N*-dimethylaniline, *N*-methyl piperazine, piperazine, and pyridine, it was found that employing Et_3N as the base yielded the most favorable results [131] (Table 3, entries 9–13). Subsequently, different quantities of Et_3N were used in the reaction to ascertain the optimal amount (Table 3, entries 14–19). The experimental data revealed that decreasing the amount of Et_3N to 0.05 mmol had a significant positive impact on the reaction. Under these conditions, the reaction achieved a substantial increase in the yield, up to 90 %, along with an improvement in the enantioselectivity, which rose to 44 %. Additionally, the reaction time was notably shortened to just 10 h (Table 3, entry 17).

Further investigation revealed that the reaction temperature also has a significant impact on the outcomes of the reaction. While decreasing the temperature resulted in a slight improvement in enantioselectivity, it also led to reduced yield and a longer reaction time. Conversely, increasing the temperature of the reaction resulted in a shorter reaction time but, unfortunately, at the expense of a noticeable decrease in both yield and enantioselectivity (Table 3, entries 20–22).

Testing different copper salts showed that $Cu(CH_3CN)_4PF_6$ was the most effective (Table 3, entries 17 vs 23–28). Other Cu (I) and Cu (II) salts resulted in a slight decrease in yield, along with poor enantioselectivity and longer reaction times. It is worth noting that, in the absence of a Cu salt, the enantioselectivity was very low, while the yield and reaction time remained acceptable (Table 3, entry 29). It was found that increasing the ratio of the ligand to $Cu(CH_3CN)_4PF_6$ had a marginal positive effect on the enantioselectivity (Table 3, entry 30). However, this improvement came at the cost of a lower yield and a longer time. Experimental outcomes were inferior when the ratio of ligand to Cu salt was reduced (Table 3, entries 31–33).

Utilizing various aromatic aldehyde derivatives under optimal conditions indicated that the presence of an electron-withdrawing group on the aromatic aldehyde improved the results, whereas electron-donating groups greatly diminished the results (Table 3, entries 17, 36 vs. 34, 35). It should be noted that neither the utilization of the heterogeneous catalyst containing a benzyl group nor the homogeneous catalysts containing nitro groups led to any significant enhancement in the yield or enantioselectivity of the corresponding product (Table 3, entries 37–41).

Considering the aforementioned optimal results, the nitroethane substrate was also investigated in the asymmetric Henry reaction utilizing both chiral homogeneous and heterogeneous ligands, $Cu(CH_3CN)_4PF_6$ and Et_3N (Table 4). It is worth noting that this reaction yielded two diastereomeric mixtures, *syn* (1*S*, 2*S*) and *anti* (1*S*, 2*R*), with the resulting products obtained in high yield, moderate enantioselectivity, and diastereoselectivity (*de* = *syn*:*anti*), with the predominant *syn* diastereomer [6,30,31,132–137].

Similar to the nitromethane reaction, the heterogeneous catalysts showed better results than the homogeneous ones. Moreover, among the homogeneous catalysts, **1a** exhibited the best efficiency. (Table 4, entries1-4). Regarding the heterogeneous catalysts, while the use of the heterogeneous catalyst containing a benzyl group resulted in the corresponding product in a slightly shorter reaction time and favorable enantioselectivity, the yield and diastereoselectivity were actually better when the heterogeneous catalyst containing a phenyl group was used (Table 4, entry 5 *vs*. 6).

Lowering the temperature could improve both *de* and *ee*; however, this improvement comes at the expense of a decrease in the yield and a longer reaction time (Table 4, entries 7 and 8). Conversely, increasing the temperature had an inverse effect (Table 4, entry 9).

Furthermore, similar to the above results, examination of different substituted aromatic aldehydes revealed that products with electron-withdrawing groups could be obtained with higher yields, *ees* and *des* (Table 4, entries 11–13).

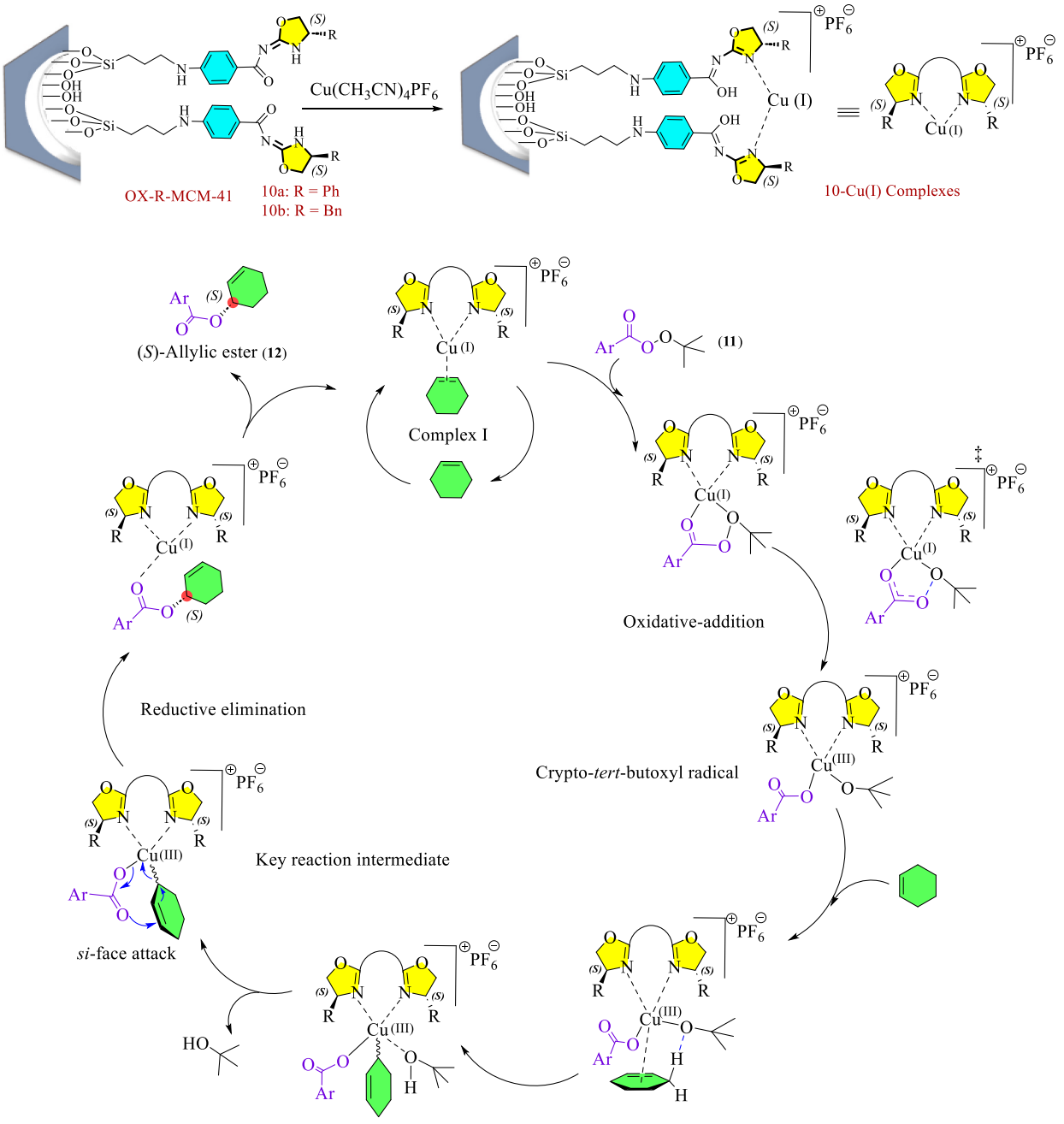

Scheme 7. Proposed mechanism of the enantioselective allylic oxidation of cyclohexene.

The catalytic cycle of the enantioselective Henry reaction, as proposed in Scheme 8, begins with the deprotonation of the nitroalkane by Et_3N at the α-carbon position, resulting in the formation of a nitronate anion, which then coordinates to the oxazoline copper complex.

Subsequently, the aldehyde coordinates to the copper atom, and in a rationalized transition state based on the obtained products (TS1), the nitronate attacks the aldehyde on the *re* face, predominantly leading to the formation of the chiral *syn*-(1*S*, 2*S*)-*β*-nitroalcohol isomer. The increased *syn*:*anti* ratio of the products can be attributed to the steric hindrance between the methyl group in the nitronate anion and the aromatic group of the aldehyde in the transition state (TS1 *vs*. TS2) [77,79,94,136,137].

Table 3
Optimizing the enantioselective Henry reaction of nitromethane under various conditions.

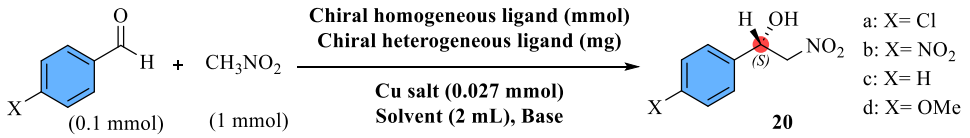

Entry	X	Base (mmol)	Ligand	Cu salt	Solvent	T (°C)	Time (h)	Yield (%)	*ee* (%)
1	Cl	Et_3N (1)	**10a** (25)	$Cu(CH_3CN)_4PF_6$	Toluene	r.t.	40	42	20
2	Cl	Et_3N (1)	**10a** (25)	$Cu(CH_3CN)_4PF_6$	CH_2Cl_2	r.t.	33	53	13
3	Cl	Et_3N (1)	**10a** (25)	$Cu(CH_3CN)_4PF_6$	THF	r.t.	22	58	22
4	Cl	Et_3N (1)	**10a** (25)	$Cu(CH_3CN)_4PF_6$	Dioxane	r.t.	20	63	27
5	Cl	Et_3N (1)	**10a** (25)	$Cu(CH_3CN)_4PF_6$	MeCN	r.t.	48	20	16
6	Cl	Et_3N (1)	**10a** (25)	$Cu(CH_3CN)_4PF_6$	EtOH	r.t.	32	71	35
7	Cl	Et_3N (1)	**10a** (25)	$Cu(CH_3CN)_4PF_6$	MeOH	r.t.	37	55	30
8	Cl	Et_3N (1)	**10a** (25)	$Cu(CH_3CN)_4PF_6$	–	r.t.	15	70	40
9	Cl	TMG (1)[a]	**10a** (25)	$Cu(CH_3CN)_4PF_6$	–	r.t.	20	68	24
10	Cl	DMA (1)[b]	**10a** (25)	$Cu(CH_3CN)_4PF_6$	–	r.t.	14	23	32
11	Cl	Piperazine (1)	**10a** (25)	$Cu(CH_3CN)_4PF_6$	–	r.t.	36	32	13
12	Cl	NMPZ(1)[c]	**10a** (25)	$Cu(CH_3CN)_4PF_6$	–	r.t.	30	25	20
13	Cl	Pyridine (1)	**10a** (25)	$Cu(CH_3CN)_4PF_6$	–	r.t.	48	43	32
14	Cl	Et_3N (0.5)	**10a** (25)	$Cu(CH_3CN)_4PF_6$	–	r.t.	16	72	36
15	Cl	Et_3N (0.25)	**10a** (25)	$Cu(CH_3CN)_4PF_6$	–	r.t.	12	80	33
16	Cl	Et_3N (0.1)	**10a** (25)	$Cu(CH_3CN)_4PF_6$	–	r.t.	12	83	38
17	Cl	Et_3N (0.05)	**10a** (25)	$Cu(CH_3CN)_4PF_6$	–	r.t.	10	90	44
18	Cl	Et_3N (0.025)	**10a** (25)	$Cu(CH_3CN)_4PF_6$	–	r.t.	18	65	40
19	Cl	Et_3N (0.01)	**10a** (25)	$Cu(CH_3CN)_4PF_6$	–	r.t.	30	48	33
20	Cl	Et_3N (0.05)	**10a** (25)	$Cu(CH_3CN)_4PF_6$	–	0	41	53	51
21	Cl	Et_3N (0.05)	**10a** (25)	$Cu(CH_3CN)_4PF_6$	–	40	8	50	8
22	Cl	Et_3N (0.05)	**10a** (25)	$Cu(CH_3CN)_4PF_6$	–	Reflux	8	10	0
23	Cl	Et_3N (0.05)	**10a** (25)	Cu_2O	–	r.t.	24	70	20
24	Cl	Et_3N (0.05)	**10a** (25)	CuCl	–	r.t.	16	75	18
25	Cl	Et_3N (0.05)	**10a** (25)	$Cu(OAc)_2$	–	r.t.	12	86	32
26	Cl	Et_3N (0.05)	**10a** (25)	$Cu(NO_3)_2$	–	r.t.	12	78	26
27	Cl	Et_3N (0.05)	**10a** (25)	$CuSO_4$	–	r.t.	24	82	12
28	Cl	Et_3N (0.05)	**10a** (25)	$CuCl_2$	–	r.t.	10	85	15
29	Cl	Et_3N (0.05)	**10a** (25)	–	–	r.t.	14	70	6
30	Cl	Et_3N (0.05)	**10a** (30)	$Cu(CH_3CN)_4PF_6$	–	r.t.	13	79	48
31	Cl	Et_3N (0.05)	**10a** (20)	$Cu(CH_3CN)_4PF_6$	–	r.t.	10	85	33
32	Cl	Et_3N (0.05)	**10a** (15)	$Cu(CH_3CN)_4PF_6$	–	r.t.	20	72	15
33	Cl	Et_3N (0.05)	**10a** (10)	$Cu(CH_3CN)_4PF_6$	–	r.t.	24	66	5
34	H	Et_3N (0.05)	**10a** (25)	$Cu(CH_3CN)_4PF_6$	–	r.t.	20	60	21
35	OMe	Et_3N (0.05)	**10a** (25)	$Cu(CH_3CN)_4PF_6$	–	r.t.	27	57	23
36	NO_2	Et_3N (0.05)	**10a** (25)	$Cu(CH_3CN)_4PF_6$	–	r.t.	5	95	50
37	NO_2	Et_3N (0.05)	**10b** (25)	$Cu(CH_3CN)_4PF_6$	–	r.t.	5	95	43
38	NO_2	Et_3N (0.05)	**1a** (0.055)	$Cu(CH_3CN)_4PF_6$	–	r.t.	2.5	85	35
39	NO_2	Et_3N (0.05)	**1b** (0.055)	$Cu(CH_3CN)_4PF_6$	–	r.t.	2.5	90	30
40	NO_2	Et_3N (0.05)	**1c** (0.055)	$Cu(CH_3CN)_4PF_6$	–	r.t.	4	85	25
41	NO_2	Et_3N (0.05)	**1d** (0.055)	$Cu(CH_3CN)_4PF_6$	–	r.t.	4	80	28

[a] Tetramethylguanidine.
[b] *N*,*N*-dimethylamine.
[c] *N*-methyl piperazine.

3. Catalyst reusability

The reusability of chiral heterogeneous catalyst **10a** in both asymmetric reactions was evaluated under optimal conditions. After completion, the catalyst was filtered, washed with CH_2Cl_2, and the resulting precipitate was dried at 50 °C. The recovered catalyst was then used for the next run of the same reaction under similar conditions. Repeating this process revealed that the activity and enantioselectivity of the heterogeneous catalyst remained relatively constant even after four consecutive cycles, demonstrating its potential for long-term application and reduced environmental impact.

Fig. 11 depicts the results for the enantioselective allylic oxidation of cyclohexene in the optimum conditions over five sequential cycles. Moreover, the XRD pattern (Fig. S33, Supplementary Material) of the catalyst after four cycles showed that the structure of the recycled catalyst did not change noticeably.

Table 4
Effect of reaction conditions on *ee* and *de* in the enantioselective Henry reaction of nitroethane.

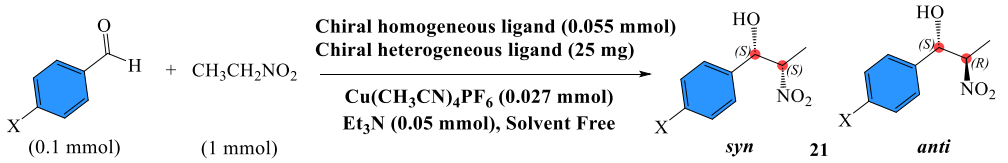

Entry	X	Ligand	T (°C)	T (h)	Yield (%)	*syn*:*anti* (%)	*ee* (%)
1	Cl	**1a**	rt	24	85	60:40	27:22
2	Cl	**1b**	rt	20	77	63:37	17:25
3	Cl	**1c**	rt	30	75	43:57	11:23
4	Cl	**1d**	rt	30	88	50:50	19:14
5	Cl	**10a**	rt	12	92	70:30	30:25
6	Cl	**10b**	rt	10	83	67:33	42:33
7	Cl	**10a**	0	27	70	73:27	40:33
8	Cl	**10a**	−10	45	46	76:24	50:43
9	Cl	**10a**	40	8	95	50:50	13:8
10	Cl	-	rt	36	75	35:65	0
11	OMe	**10a**	rt	18	75	62:38	17:23
12	H	**10a**	rt	20	80	70:30	29:20
13	NO_2	**10a**	rt	5	95	78:22	43:37

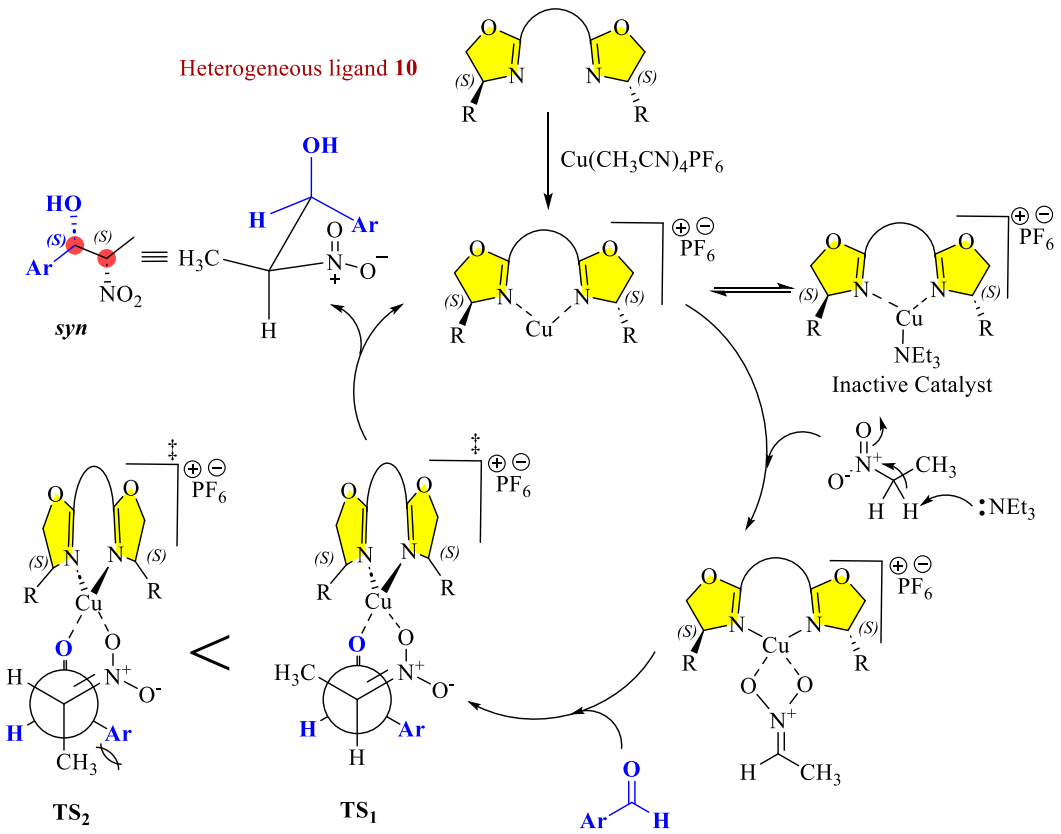

Scheme 8. Plausible mechanism of the enantioselective Henry reaction.

4. Conclusions

In summary, we successfully prepared and characterized a class of recyclable heterogeneous oxazoline-based ligands by immobilizing synthesized chiral amido-oxazoline on MCM-41 mesoporous silica. The performance of these chiral heterogeneous ligands was

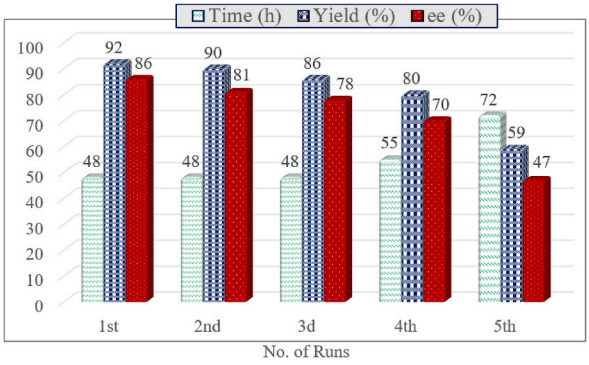

Fig. 11. Reusability of catalyst **10a** in the enantioselective allylic oxidation of cyclohexene.

evaluated in two enantioselective reactions: the allylic oxidation of olefins and the Henry reaction. In both cases, heterogeneous catalyst outperformed their homogeneous counterparts in terms of enantioselectivity. Significantly, the enantioselective Henry reaction proceeded efficiently under solvent-free conditions, aligning with green chemistry principles. Additionally, the use of nitroethane in the Henry reaction yielded predominantly the *syn* diastereomer. Future investigations will explore immobilization on alternative supports such as SBA-15 and MOFs, with the aim of optimizing reaction conditions and broadening the scope of these heterogeneous catalysts.

CRediT authorship contribution statement

Niloofar Tavakoli: Methodology, Investigation, Formal analysis. **Hamid Arvinnezhad:** Writing – original draft, Methodology, Investigation, Formal analysis. **Shiva Majidian:** Methodology, Investigation, Formal analysis. **Mahsa Mahramasrar:** Methodology, Investigation, Formal analysis. **Khosrow Jadidi:** Supervision, Methodology, Investigation, Formal analysis, Conceptualization. **Saadi Samadi:** Writing – original draft, Supervision, Methodology, Investigation, Formal analysis, Conceptualization.

Declaration of generative AI and AI-assisted technologies in the writing process

During the preparation of this work the authors used GPT3.5 in order to improve writing. After using this service, the authors reviewed and edited the content as needed and take full responsibility for the content of the publication.

Declaration of competing interest

The authors declare that they have no known competing financial interests or personal relationships that could have appeared to influence the work reported in this paper.

Acknowledgements

The authors are grateful to the University of Kurdistan Research Councils and the Iran National Science Foundation (Project No: 4003026) for providing financial support for this research.

Appendix A. Supplementary data

Supplementary data to this article can be found online at https://doi.org/10.1016/j.heliyon.2024.e39911.

References

[1] P. Braunstein, F. Naud, Hemilability of hybrid ligands and the coordination chemistry of oxazoline-based systems, Angew. Chem. Int. Ed. 40 (2001) 680–699.
[2] M. Gómez, G. Muller, M. Rocamora, Coordination chemistry of oxazoline ligands, Coord. Chem. Rev. 193 (1999) 769–835.
[3] J.L. Cryder, A.J. Killgore, C. Moore, J.A. Golen, A.L. Rheingold, C.J. Daley, Novel metal complexes containing a chiral trinitrogen isoindoline-based pincer ligand: *in situ* synthesis and structural characterization, Dalton Trans. 39 (2010) 10671–10677.
[4] J.M. Fraile, J.I. García, C.I. Herrerías, J.A. Mayoral, O. Reiser, A. Socuéllamos, H. Werner, The role of binding constants in the efficiency of chiral catalysts immobilized by electrostatic interactions: the case of azabis (oxazoline)–copper complexes, Chem. Eur. J. 10 (2004) 2997–3005.
[5] A. Gissibl, M. Finn, O. Reiser, Cu(II)-Aza (bisoxazoline)-catalyzed asymmetric benzoylations, Org. Lett. 7 (2005) 2325–2328.
[6] K. Lang, J. Park, S. Hong, Development of bifunctional aza-bis (oxazoline) copper catalysts for enantioselective henry reaction, J. Org. Chem. 75 (2010) 6424–6435.

[7] C.O. Kangani, D.E. Kelley, B.W. Day, One pot direct synthesis of oxazolines, benzoxazoles, and oxadiazoles from carboxylic acids using the Deoxo-Fluor reagent, Tetrahedron Lett. 47 (2006) 6497–6499.
[8] P. Wipf, S. Venkatraman, From aziridines to oxazolines and thiazolines: the heterocyclic route to thiangazole, Synlett 1 (1997) 1–10.
[9] P.G. Wuts, J.M. Northuis, T.A. Kwan, The synthesis of oxazolines using the Vilsmeier reagent, J. Org. Chem. 65 (2000) 9223–9225.
[10] G. Desimoni, G. Faita, K.A. Jørgensen, Update 1 of: C_2-Symmetric chiral bis(oxazoline) ligands in asymmetric catalysis, Chem. Rev. 111 (2011) PR284–PR437.
[11] G. Desimoni, G. Faita, K.A. Jørgensen, C_2-Symmetric chiral bis(oxazoline) ligands in asymmetric catalysis, Chem. Rev. 106 (2006) 3561–3651.
[12] S. Samadi, H. Arvinnezhad, S. Mansoori, H. Parsa, Preparation and DFT studies of chiral Cu (I)-complexes of biphenyl bisoxazolines and their application in enantioselective Kharasch–Sosnovsky reaction, Sci. Rep. 12 (2022), 15038-11550.
[13] M. Benaglia, Recoverable and Recyclable Catalysts, John Wiley & Sons, 2009.
[14] M. Pagliaro, Silica-Based Materials for Advanced Chemical Applications, Royal Society of Chemistry, 2009.
[15] Z. Yang, Y. Lu, Z. Yang, Mesoporous materials: tunable structure, morphology and composition, Chem. Commun. (2009) 2270–2277.
[16] J.C. Vartuli, K.D. Schmitt, C.T. Kresge, W. Roth, M.E. Leonowicz, S.B. McCullen, S.D. Hellring, J.S. Beck, J.L. Schlenker, Effect of surfactant/silica molar ratios on the formation of mesoporous molecular sieves: inorganic mimicry of surfactant liquid-crystal phases and mechanistic implications, Chem. Mater. 6 (1994) 2317–2326.
[17] C.D. Nunes, A.A. Valente, M. Pillinger, A.C. Fernandes, C.C. Romão, J. Rocha, I.S. Gonçalves, MCM-41 functionalized with bipyridyl groups and its use as a support for oxomolybdenum (VI) catalysts, J. Mater. Chem. 12 (2002) 1735–1742.
[18] D. Kumar, K. Schumacher, C.D.F. Von Hohenesche, M. Grün, K. Unger, MCM-41, MCM-48 and related mesoporous adsorbents: their synthesis and characterisation, Colloids Surf. A: Physicochem. Eng. Asp. 187 (2001) 109–116.
[19] L. Bois, A. Bonhommé, A. Ribes, B. Pais, G. Raffin, F. Tessier, Functionalized silica for heavy metal ions adsorption, Colloids Surf. A: Physicochem. Eng. Asp. 221 (2003) 221–230.
[20] C. Lesaint, B. Lebeau, C. Marichal, J. Patarin, Synthesis of mesoporous silica materials functionalized with *n*-propyl groups, Micropor. Mesopor. Mater. 83 (2005) 76–84.
[21] K. Aghapoor, M.M. Amini, K. Jadidi, F. Mohsenzadeh, H.R. Darabi, Catalytic activity of the nanoporous MCM-41 surface for the Paal–Knorr pyrrole cyclocondensation, Z. Naturforsch. B 70 (2015) 475–481.
[22] C.E. Song, S.-g. Lee, Supported chiral catalysts on inorganic materials, Chem. Rev. 102 (2002) 3495–3524.
[23] J.M. Fraile, J.I. García, J.A. Mayoral, E. Pires, Heterogenization on inorganic supports: methods and applications, in: P. Barbaro, F. Liguori (Eds.), Heterogenized Homogeneous Catalysts for Fine Chemicals Production: Materials and Processes, 2010, pp. 65–121.
[24] R.I. Kureshy, I. Ahmad, H.K. Noor-ul, S.H. Abdi, K. Pathak, R.V. Jasra, Chiral Mn (III) salen complexes covalently bonded on modified MCM-41 and SBA-15 as efficient catalysts for enantioselective epoxidation of nonfunctionalized alkenes, J. Catal. 238 (2006) 134–141.
[25] C. Li, H. Zhang, D. Jiang, Q. Yang, Chiral catalysis in nanopores of mesoporous materials, Chem. Commun. (2007) 547–558.
[26] J. Dupont, R.F. de Souza, P.A. Suarez, Ionic liquid (molten salt) phase organometallic catalysis, Chem. Rev. 102 (2002) 3667–3692.
[27] Q.-H. Fan, Y.-M. Li, A.S. Chan, Recoverable catalysts for asymmetric organic synthesis, Chem. Rev. 102 (2002) 3385–3466.
[28] D.E. Bergbreiter, J. Tian, C. Hongfa, Using soluble polymer supports to facilitate homogeneous catalysis, Chem. Rev. 109 (2009) 530–582.
[29] J.M. Fraile, J.I. García, C.I. Herrerías, J.A. Mayoral, E. Pires, Enantioselective catalysis with chiral complexes immobilized on nanostructured supports, Chem. Soci. Rev. 38 (2009) 695–706.
[30] R. Maggi, D. Lanari, C. Oro, G. Sartori, L. Vaccaro, Heterogeneous bisoxazoline/copper complex: a green catalyst for the enantioselective reaction of nitromethane with substituted benzaldehydes, Eur. J. Org. Chem. 2011 (2011) 5551–5554.
[31] J.-M. Lee, J. Kim, Y. Shin, C.-E. Yeom, J.E. Lee, T. Hyeon, B.M. Kim, Heterogeneous asymmetric Henry reaction using a chiral bis (oxazoline)-copper complex immobilized on magnetically separable mesocellular mesoporous silica support, Tetrahedron: Asymmetry 21 (2010) 285–291.
[32] J. Eames, M. Watkinson, Catalytic allylic oxidation of alkenes using an asymmetric Kharasch–Sosnovsky reaction, Angew. Chem. Int. Ed. 40 (2001) 3567–3571.
[33] M.B. Andrus, J.C. Lashley, Copper catalyzed allylic oxidation with peresters, Tetrahedron 58 (2002) 845–866.
[34] A.L. García-Cabeza, F.J. Moreno-Dorado, M.J. Ortega, F.M. Guerra, Copper-catalyzed oxidation of alkenes and heterocycles, Synthesis 48 (2016) 2323–2342.
[35] S. Samadi, H. Arvinnezhad, S. Nazari, S. Majidian, Enantioselective allylic C–H bond oxidation of olefins using copper complexes of chiral oxazoline based ligands, Top. Curr. Chem. 380 (2022) 20.
[36] L. Aldea, I. Delso, M. Hager, M. Glos, J.I. García, J.A. Mayoral, O. Reiser, A reusable enantioselective catalytic system for the Kharasch–Sosnovsky allylic oxidation of alkenes based on a ditopic azabis (oxazoline) ligand, Tetrahedron 68 (2012) 3417–3422.
[37] A.S. Gokhale, A.B. Minidis, A. Pfaltz, Enantioselective allylic oxidation catalyzed by chiral bisoxazoline-copper complexes, Tetrahedron Lett. 36 (1995) 1831–1834.
[38] M.B. Andrus, A.B. Argade, X. Chen, M.G. Pamment, The asymmetric Kharasch reaction. Catalytic enantioselective allylic acyloxylation of olefins with chiral copper (I) complexes and *tert*-butyl perbenzoate, Tetrahedron Lett. 36 (1995) 2945–2948.
[39] M.B. Andrus, X. Chen, Catalytic enantioselective allylic oxidation of olefins with copper (I) catalysts and new perester oxidants, Tetrahedron 53 (1997) 16229–16240.
[40] K. Kawasaki, S. Tsumura, T. Katsuki, Enantioselective allylic oxidation using biomimetic tris (oxazolines)-copper (II) complex, Synlett 1995 (1995) 1245–1246.
[41] Y. Kohmura, T. Katsuki, Asymmetric allylic oxidation of cycloalkenes using a tridentate tris (oxazoline) ligand as a chiral auxiliary, Tetrahedron Lett. 41 (2000) 3941–3945.
[42] A. DattaGupta, V.K. Singh, Catalytic enantioselective allylic oxidation of olefins with copper complexes of chiral nonracemic bis (oxazolinyl) pyridine type ligands, Tetrahedron Lett. 37 (1996) 2633–2636.
[43] G. Sekar, A. DattaGupta, V.K. Singh, Asymmetric Kharasch reaction: catalytic enantioselective allylic oxidation of olefins using chiral pyridine bis (diphenyloxazoline)− copper complexes and *tert*-butyl perbenzoate, J. Org. Chem. 63 (1998) 2961–2967.
[44] S.K. Ginotra, V.K. Singh, Enantioselective oxidation of olefins catalyzed by chiral copper bis (oxazolinyl) pyridine complexes: a reassessment, Tetrahedron 62 (2006) 3573–3581.
[45] S.K. Ginotra, V.K. Singh, Studies on enantioselective allylic oxidation of olefins using peresters catalyzed by Cu (I)-complexes of chiral pybox ligands, Org. Biomol. Chem. 4 (2006) 4370–4374.
[46] P.K. Singh, V.K. Singh, Enantioselective reactions catalyzed by chiral pyridine 2, 6-bis (5', 5'-diphenyloxazoline)-metal complexes, Pure Appl. Chem. 82 (2010) 1845–1853.
[47] M.B. Andrus, Z. Zhou, Highly enantioselective copper− bisoxazoline-catalyzed allylic oxidation of cyclic olefins with *tert*-butyl *p*-nitroperbenzoate, J. Am. Chem. Soc. 124 (2002) 8806–8807.
[48] J. Thorhauge, M. Roberson, R.G. Hazell, K.A. Jørgensen, On the intermediates in chiral bis (oxazoline) copper (II)-catalyzed enantioselective reactions: experimental and theoretical investigations, Chem. Eur J. 8 (2002) 1888–1898.
[49] J.S. Johnson, D.A. Evans, Chiral bis (oxazoline) copper (II) complexes: versatile catalysts for enantioselective cycloaddition, aldol, Michael, and carbonyl ene reactions, Acc. Chem. Res. 33 (2000) 325–335.
[50] Z. Zhou, M.B. Andrus, Naphthyl-substituted bisoxazoline and pyridylbisoxazoline–copper (I) catalysts for asymmetric allylic oxidation, Tetrahedron Lett. 53 (2012) 4518–4521.
[51] J. áStephen Clark, K. Tolhurst, Enantioselective allylic acyloxylation catalysed by copper–oxazoline complexes, J. Chem. Soc., Perkin Trans. 1 (1998) 1167–1170.
[52] B. Liu, S.-F. Zhu, L.-X. Wang, Q.-L. Zhou, Preparation and application of bisoxazoline ligands with a chiral spirobiindane skeleton for asymmetric cyclopropanation and allylic oxidation, Tetrahedron: Asymmetry 17 (2006) 634–641.

[53] V. Köhler, C. Mazet, A. Toussaint, K. Kulicke, D. Häussinger, M. Neuburger, S. Schaffner, S. Kaiser, A. Pfaltz, Chiral boron-bridged bisoxazoline (Borabox) ligands: structures and reactivities of Pd and Cu complexes, Chem. Eur J. 14 (2008) 8530–8539.
[54] S. Samadi, A. Ashouri, H.I. Rashid, S. Majidian, M. Mahramasrar, Immobilization of (L)-valine and (L)-valinol on SBA-15 nanoporous silica and their application as chiral heterogeneous ligands in the Cu-catalyzed asymmetric allylic oxidation of alkenes, New J. Chem. 45 (2021) 17630–17641.
[55] A. Rezaei, H. Zheng, S. Majidian, S. Samadi, A. Ramazani, Chiral pseudohomogeneous catalyst based on amphiphilic carbon quantum dots for the enantioselective Kharasch–Sosnovsky reaction, ACS Appl. Mater. Interfaces 15 (2023) 54373–54385.
[56] K. Akutu, H. Kabashima, T. Seki, H. Hattori, Nitroaldol reaction over solid base catalysts, Appl. Catal. A: Gen. 247 (2003) 65–74.
[57] A. Alizadeh, M.M. Khodaei, G. Abdi, D. Kordestani, The first report on chemoselective biguanide-catalyzed Henry reaction under neat conditions, Bull. Korean Chem. Soc. 33 (2012) 3640–3644.
[58] T. Arai, M. Watanabe, A. Yanagisawa, Practical Asymmetric Henry reaction catalyzed by a chiral diamine-Cu(OAc)$_2$ complex, Org. Lett. 9 (2007) 3595–3597.
[59] H. Li, B. Wang, L. Deng, Enantioselective nitroaldol reaction of α-ketoesters catalyzed by Cinchona alkaloids, J. Am. Chem. Soc. 128 (2006) 732–733.
[60] N. Gogoi, J. Boruwa, N.C. Barua, A total synthesis of (−)-bestatin using Shibasaki's asymmetric Henry reaction, Tetrahedron Lett. 46 (2005) 7581–7582.
[61] J. Blacker, Catalytic asymmetric synthesis. Iwao Ojima Wiley− VCH, ACS Publications, New York, 2001.
[62] D.J. Ager, I. Prakash, D.R. Schaad, 1,2-Amino alcohols and their heterocyclic derivatives as chiral auxiliaries in asymmetric synthesis, Chem. Rev. 96 (1996) 835–876.
[63] M. Shibasaki, H. Groger, M. Kanai, Nitroaldol reaction, in: E.N. Jacobsen, A. Pfaltz, H. Yamamoto (Eds.), Comprehensive Asymmetric Catalysis: Supplement 1, Springer Science & Business Media, 2003.
[64] C. Palomo, M. Oiarbide, A. Laso, Recent advances in the catalytic asymmetric nitroaldol (Henry) reaction, Eur. J. Org. Chem. 2007 (2007) 2561–2574.
[65] J. Park, K. Lang, K.A. Abboud, S. Hong, Self-assembled dinuclear cobalt (II)-salen catalyst through hydrogen-bonding and its application to enantioselective nitro-aldol (Henry) reaction, J. Amer. Chem. Soc. 130 (2008) 16484–16485.
[66] B. Qin, Xiao, X. Liu, J. Huang, Y. Wen, X. Feng, Highly enantioselective Henry (nitroaldol) reaction of aldehydes and α-ketoesters catalyzed by *N,N'*-dioxide-copper(I) complexes, J. Org. Chem. 72 (2007) 9323–9328.
[67] T. Ooi, K. Doda, K. Maruoka, Designer chiral quaternary ammonium bifluorides as an efficient catalyst for asymmetric nitroaldol reaction of silyl nitronates with aromatic aldehydes, J. Am. Chem. Soc. 125 (2003) 2054–2055.
[68] C. Palomo, M. Oiarbide, A. Mielgo, Unveiling reliable catalysts for the asymmetric nitroaldol (Henry) reaction, Angew. Chem. Int. Ed. 43 (2004) 5442–5444.
[69] B.M. Choudary, K.V. Ranganath, U. Pal, M.L. Kantam, B. Sreedhar, Nanocrystalline MgO for asymmetric henry and michael reactions, J. Amer. Chem. Soc. 127 (2005) 13167–13171.
[70] B.M. Trost, V.S. Yeh, A dinuclear Zn catalyst for the asymmetric nitroaldol (Henry) reaction, Angew. Chem. 114 (2002) 889–891.
[71] J. Boruwa, N. Gogoi, P.P. Saikia, N.C. Barua, Catalytic asymmetric Henry reaction, Tetrahedron: Asymmetry 17 (2006) 3315–3326.
[72] H. Sasai, T. Suzuki, S. Arai, T. Arai, M. Shibasaki, Basic character of rare earth metal alkoxides. Utilization in catalytic carbon-carbon bond-forming reactions and catalytic asymmetric nitroaldol reactions, J. Am. Chem. Soc. 114 (1992) 4418–4420.
[73] T. Risgaard, K.V. Gothelf, K.A. Jørgensen, Catalytic asymmetric Henry reactions of silyl nitronates with aldehydes, Org. Biomol. Chem. 1 (2003) 153–156.
[74] A. Chougnet, G. Zhang, K. Liu, D. Häussinger, A. Kägi, T. Allmendinger, W.D. Woggon, Diastereoselective and highly enantioselective Henry reactions using C_1-symmetrical copper (II) complexes, Adv. Synth. Catal. 353 (2011) 1797–1806.
[75] G. Blay, V. Hernandez-Olmos, J.R. Pedro, Development of new *N, N*-ligands for the enantioselective copper (II)-catalyzed Henry reaction, Synlett 2011 (2011) 1195–1211.
[76] C. Gan, G. Lai, Z. Zhang, Z. Wang, M.-M. Zhou, Efficient and enantioselective nitroaldol reaction catalyzed by copper Schiff-base complexes, Tetrahedron: Asymmetry 17 (2006) 725–728.
[77] D.A. Evans, D. Seidel, M. Rueping, H.W. Lam, J.T. Shaw, C.W. Downey, A new copper acetate-bis(oxazoline)-catalyzed, enantioselective Henry reaction, J. Am. Chem. Soc. 125 (2003) 12692–12693.
[78] C. Christensen, K. Juhl, K.A. Jørgensen, Catalytic asymmetric Henry reactions. A simple approach to optically active β-nitro α-hydroxy esters, Chem. Commun. (2001) 2222–2223.
[79] C. Christensen, K. Juhl, R.G. Hazell, K.A. Jørgensen, Copper-catalyzed enantioselective Henry reactions of α-keto esters: an easy entry to optically active β-nitro-α-hydroxy esters and β-amino-α-hydroxy esters, J. Org. Chem. 67 (2002) 4875–4881.
[80] R.B. Kawthekar, S.K. Chakka, V. Francis, P.G. Andersson, H.G. Kruger, G.E. Maguire, T. Govender, Synthesis of tetrahydroisoquinoline (TIQ)–oxazoline ligands and their application in enantioselective Henry reactions, Tetrahedron: Asymmetry 21 (2010) 846–852.
[81] E. Wolińska, Chiral oxazoline ligands containing a 1, 2, 4-triazine ring and their application in the Cu-catalyzed asymmetric Henry reaction, Tetrahedron 69 (2013) 7269–7278.
[82] W. Yang, H. Liu, D.-M. Du, Efficient in situ three-component formation of chiral oxazoline-Schiff base copper (II) complexes: towards combinatorial library of chiral catalysts for asymmetric Henry reaction, Org. Biomol. Chem. 8 (2010) 2956–2960.
[83] H. Sasai, 2.13 the henry (nitroaldol) reaction, in: P. Knochel (Ed.), Comprehensive Organic Synthesis, second ed., Elsevier, Amsterdam, 2014, pp. 543–570.
[84] S. Chandrasekhar, A. Shrinidhi, Useful extensions of the Henry reaction: expeditious routes to nitroalkanes and nitroalkenes in aqueous media, Synth. Commun. 44 (2014) 3008–3018.
[85] R.S. Varma, R. Dahiya, S. Kumar, Microwave-assisted Henry reaction: solventless synthesis of conjugated nitroalkenes, Tetrahedron Lett. 38 (1997) 5131–5134.
[86] The nitro-aldol (henry) reaction, in: The Nitro Group in Organic Synthesis, Wiley− VCH, 2001, pp. 30–69.
[87] H.Y. Kim, K. Oh, Brucine-derived amino alcohol catalyzed asymmetric Henry reaction: an orthogonal enantioselectivity approach, Org. Lett. 11 (2009) 5682–5685.
[88] P.M. Koskinen, A.M. Koskinen, Sphingosine, an enigmatic lipid: a review of recent literature syntheses, Synthesis 1998 (1998) 1075–1091.
[89] D. Lednicer, The Organic Chemistry of Drug Synthesis, ume 7, John Wiley & Sons, 2007.
[90] F.A. Luzzio, The Henry reaction: recent examples, Tetrahedron 57 (2001) 915–945.
[91] H. Sasai, N. Itoh, T. Suzuki, M. Shibasaki, Catalytic asymmetric nitroaldol reaction: an efficient synthesis of (*S*) propranolol using the lanthanum binaphthol complex, Tetrahedron Lett. 34 (1993) 855–858.
[92] H. Sasai, Y.M. Yamada, T. Suzuki, M. Shibasaki, Syntheses of (*S*)-(−)-pindolol and [3′-13C]-(*R*)-(−)-pindolol utilizing a lanthanum-lithium-(*R*)-BINOL ((*R*)-LLB) catalyzed nitroaldol reaction, Tetrahedron 50 (1994) 12313–12318.
[93] H. Sasai, T. Suzuki, N. Itoh, S. Arai, M. Shibasaki, Effects of rare earth metals on the catalytic asymmetric nitroaldol reaction, Tetrahedron Lett. 34 (1993) 2657–2660.
[94] J.D. White, S. Shaw, A new catalyst for the asymmetric Henry reaction: synthesis of β-nitroethanols in high enantiomeric excess, Org. Lett. 14 (2012) 6270–6273.
[95] B.M. Trost, V.S. Yeh, H. Ito, N. Bremeyer, Effect of ligand structure on the zinc-catalyzed Henry reaction. Asymmetric syntheses of (−)-denopamine and (−)-arbutamine, Org. Lett. 4 (2002) 2621–2623.
[96] S. Samadi, K. Jadidi, M. Samadi, A. Ashouri, B. Notash, Designing chiral amido-oxazolines as new chelating ligands devoted to direct Cu-catalyzed oxidation of allylic C-H bonds in cyclic olefins, Tetrahedron 75 (2019) 862–867.
[97] M.J. McKennon, A. Meyers, K. Drauz, M. Schwarm, A convenient reduction of amino acids and their derivatives, J. Org. Chem. 58 (1993) 3568–3571.
[98] S. Samadi, A. Ashouri, M. Samadi, Synthesis of chiral allylic esters by using the new recyclable chiral heterogeneous oxazoline-based catalysts, ACS Omega 5 (2020) 22367–22378.
[99] J. Morris, L. Kovács, Ohe K., Cyanogen bromide, in: A. Charette, J. Bode, T. Rovis, R. Shenvi (Eds.), Encyclopedia of Reagents for Organic Synthesis, John Wiley & Sons, 2005, pp. 1-8..
[100] C. Agami, S. Cheramy, L. Dechoux, M. Melaimi, Enantioselective synthesis of α, β-substituted β-amino acids, Tetrahedron 57 (2001) 195–200.

[101] S. Ueda, H. Terauchi, A. Yano, M. Ido, M. Matsumoto, M. Kawasaki, 4, 5-Disubstituted-1, 3-oxazolidin-2-imine derivatives: a new class of orally bioavailable nitric oxide synthase inhibitor, Bioorg. Med. Chem. Lett. 14 (2004) 313–316.
[102] S.-J. Jia, D.-M. Du, Enantioselective chlorination of β-keto esters and amides catalyzed by chiral copper (II) complexes of squaramide-linked bisoxazoline ligand, Chin. Chem. Lett. 25 (2014) 1479–1484.
[103] M. Glos, O. Reiser, Aza-bis (oxazolines): new chiral ligands for asymmetric catalysis, Org. Lett. 2 (2000) 2045–2048.
[104] H. Werner, R. Vicha, A. Gissibl, O. Reiser, Improved synthesis of aza-bis (oxazoline) ligands, J. Org. Chem. 68 (2003) 10166–10168.
[105] G. Galley, A.l. Beurier, G. Décoret, A. Goergler, R. Hutter, S. Mohr, A. Pahler, P. Schmid, D. Turck, R. Unger, Discovery and characterization of 2-aminooxazolines as highly potent, selective, and orally active TAAR1 agonists, ACS Med. Chem. Lett. 7 (2016) 192–197.
[106] L.K. Pilsl, T. Ertl, O. Reiser, Enantioselective three-step synthesis of homo-β-proline: a donor–acceptor cyclopropane as key intermediate, Org. Lett. 19 (2017) 2754–2757.
[107] F. Mu, S.L. Coffing, D.J. Riese, R.L. Geahlen, P. Verdier-Pinard, E. Hamel, J. Johnson, M. Cushman, Design, synthesis, and biological evaluation of a series of lavendustin A analogues that inhibit EGFR and Syk tyrosine kinases, as well as tubulin polymerization, J. Med. Chem. 44 (2001) 441–452.
[108] S. Samadi, K. Jadidi, B. Khanmohammadi, N. Tavakoli, Heterogenization of chiral mono oxazoline ligands by grafting onto mesoporous silica MCM-41 and their application in copper-catalyzed asymmetric allylic oxidation of cyclic olefins, J. Catal. 340 (2016) 344–353.
[109] S. Samadi, S. Nazari, H. Arvinnezhad, K. Jadidi, B. Notash, A significant improvement in enantioselectivity, yield, and reactivity for the copper-bi-*o*-tolyl bisoxazoline-catalyzed asymmetric allylic oxidation of cyclic olefins using recoverable SBA-15 mesoporous silica material, Tetrahedron 69 (2013) 6679–6686.
[110] P.H. Gore, S. Thorburn, D.J. Weyell, Friedel–Crafts reactions. Part XXV. Acetylation and benzoylation of iodobenzene and of *o*-, *m*-, and *p*-iodotoluenes, J. Chem. Soc., Perkin Trans. 1 (1973) 2940–2948.
[111] S. Samadi, A. Ashouri, S. Kamangar, F. Pourakbari, 2-Aminopyrazine-functionalized MCM-41 nanoporous silica as a new efficient heterogeneous ligand for Cu-catalyzed allylic C–H bonds oxidation of olefins, Res. Chem. Intermed. 46 (2020) 557–569.
[112] J.C. Dore, R.E. Benfield, D. Grandjean, G. Schmid, M. Kröll, D. Le Bolloc'h, Structural studies of mesoporous alumina membranes by small angle X-ray scattering, in: F. Rodriguez-Reinoso, B. McEnaney, J. Rouquerol, K. Unger (Eds.), Studies in Surface Science and Catalysis, Elsevier, 2002, pp. 163–170.
[113] Z.A. ALOthman, A review: fundamental aspects of silicate mesoporous materials, Materials 5 (2012) 2874–2902.
[114] S. Samadi, K. Jadidi, B. Notash, Chiral bisoxazoline ligands with a biphenyl backbone: development and application in catalytic asymmetric allylic oxidation of cycloolefins, Tetrahedron: Asymmetry 24 (2013) 269–277.
[115] F. Anet, L. Kozerski, Determination of conformational barriers in 1, 5-cyclooctadiene by proton and carbon-13 nuclear magnetic resonance, J. Am. Chem. Soc. 95 (1973) 3407–3408.
[116] F.A. Anet, N.R. Easton Jr., I. Yavari, Carbon-13 nuclear magnetic resonance spectra and conformations of *cis, cis*-1, 5-cyclooctadiene monoepoxide and *cis, syn, cis*-1, 5-cyclooctadiene diepoxide, Org. Magn. Reson. 12 (1979) 299–301.
[117] F. Sauriol-Lord, M. St-Jacques, Stereodynamic investigation of dibenzo-1, 5-cyclooctadiene and 5, 6, 11, 12-tetrahydrodibenzo [*b, f*][1, 4] diazocine derivatives, Can. J. Chem. 53 (1975) 3768–3776.
[118] Z. Sehhat, S. Mansoori, H. Arvinnezhad, Y. Naghdi, S. Samadi, Application of chiral Betti base-copper complexes in enantioselective allylic oxidation of olefins, computational studies of the Betti bases, and docking of the resulting chiral allylic esters, Mol. Catal. 538 (2023) 113011.
[119] A.L. Beckwith, A.A. Zavitsas, Allylic oxidations by peroxy esters catalyzed by copper salts. The potential for stereoselective syntheses, J. Am. Chem. Soc. 108 (1986) 8230–8234.
[120] J. Kochi, The mechanism of the copper salt catalysed reactions of peroxides, Tetrahedron 18 (1962) 483–497.
[121] J. Kochi, R. Subramanian, Kinetics of electron-transfer oxidation of alkyl radicals by copper (II) complexes, J. Am. Chem. Soc. 87 (1965) 4855–4866.
[122] J.K. Kochi, Copper salt-catalyzed reaction of butenes with peresters, J. Am. Chem. Soc. 84 (1962) 774–784.
[123] J.K. Kochi, P.J. Krusic, Isomerization and electron spin resonance of allylic radicals, J. Am. Chem. Soc. 90 (1968) 7157–7159.
[124] K. Smith, C.D. Hupp, K.L. Allen, G.A. Slough, Catalytic allylic amination versus allylic oxidation: a mechanistic dichotomy, Organometallics 24 (2005) 1747–1755.
[125] C. Walling, W. Thaler, Positive halogen compounds. III. Allylic chlorination with *t*-butyl hypochlorite the stereochemistry of allylic radicals1, J. Am. Chem. Soc. 83 (1961) 3877–3884.
[126] C. Walling, A.A. Zavitsas, The copper-catalyzed reaction of peresters with hydrocarbons, J. Am. Chem. Soc. 85 (1963) 2084–2090.
[127] N. Zhu, B. Qian, H. Xiong, H. Bao, Copper-catalyzed regioselective allylic oxidation of olefins via C–H activation, Tetrahedron Lett. 58 (2017) 4125–4128.
[128] J.A. Mayoral, S. Rodríguez-Rodríguez, L. Salvatella, Theoretical insights into enantioselective catalysis: the mechanism of the Kharasch–Sosnovsky reaction, Chem. Eur J. 14 (2008) 9274–9285.
[129] J. Fan, G. Sun, C. Wan, Z. Wang, Y. Li, Investigation of DNA as a catalyst for Henry reaction in water, Chem. Commun. (2008) 3792–3794.
[130] A.E. Aydin, S. Yuksekdanaci, Asymmetric Henry reactions catalyzed by metal complexes of chiral oxazoline based ligands, Tetrahedron: Asymmetry 24 (2013) 14–22.
[131] M. Mahramasrar, S. Rezajo, S. Majidian, B. Rostami Tabesh, S. Samadi, Enhancing catalytic activity of UiO-66 through CuO nanoparticles incorporation: a study on Henry reaction and one-pot allylic C-H bond oxidation of olefins, J. Chem. Sci. 136 (2024) 25.
[132] V.J. Bulbule, V.H. Deshpande, S. Velu, A. Sudalai, S. Sivasankar, V. Sathe, Heterogeneous Henry reaction of aldehydes: diastereoselective synthesis of nitroalcohol derivatives over Mg-Al hydrotalcites, Tetrahedron 55 (1999) 9325–9332.
[133] Z.H. Li, Z.M. Zhou, X.Y. Hao, J. Zhang, X. Dong, Y.Q. Liu, Noncovalent immobilization of ionic tagged Box-Cu$(OAc)_2$ complex and its application in asymmetric Henry reaction, Chirality 24 (2012) 1092–1095.
[134] M. Gaab, S. Bellemin-Laponnaz, L.H. Gade, Catalysis in a Tea Bag: synthesis, catalytic performance and recycling of dendrimer-immobilised bis-and trisoxazoline copper catalysts, Chem. Eur. J. 15 (2009) 5450–5462.
[135] A. Gualandi, L. Cerisoli, H. Stoeckli-Evans, D. Savoia, Pyrrole macrocyclic ligands for Cu-catalyzed asymmetric Henry reactions, J. Org. Chem. 76 (2011) 3399–3408.
[136] W. Jin, X. Li, B. Wan, A highly diastereo-and enantioselective copper (I)-catalyzed henry reaction using a bis (sulfonamide)-diamine ligand, J. Org. Chem. 76 (2011) 484–491.
[137] S.K. Ginotra, V.K. Singh, Enantioselective Henry reaction catalyzed by a C_2-symmetric bis (oxazoline)–Cu $(OAc)_2 \cdot H_2O$ complex, Org. Biomol. Chem. 5 (2007) 3932–3937.